Magnetic anisotropy and orbital magnetism

Klaus Baberschke

Institut für Experimentalphysik
Freie Universität Berlin
Arnimallee 14   D-14195 Berlin-Dahlem   Germany

1. **Introduction (tutorial)**

2. **Magnetic Anisotropy Energy (MAE)**

3. **Orbital magnetic moment μ_L**
   (which technique measures what?)

$\Rightarrow$ **http://www.physik.fu-berlin.de/~ag-baberschke**

1. Introduction

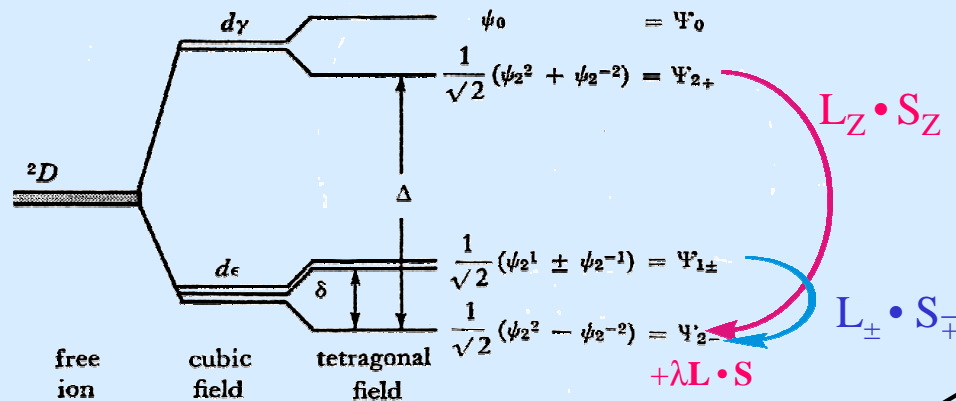Für einen 3d^1 Zustand mit MX$_6$ Liganden ist die Energieaufspaltung in tetragonaler Symmetrie wie folgt gegeben:

Fig. 3-4 Splitting of the ^2D term by a tetragonally distorted cubic field.

The orbital moment is quenched in cubic symmetry

$$\langle 2\text{-}|\,L_Z\,|\,2\text{-}\rangle = 0,$$

but not for tetragonal symmetry

3) Berechnen Sie für den Grundzustand

$$\psi_{2-} \equiv (2)^{-1/2}\{|2> - |-2>\} \equiv |2->$$

die Beimischung der angeregten Zustände durch $\lambda \mathbf{L}\cdot\mathbf{S}$ und beachten Sie dabei, daß auch Spinzustände einzuführen sind (zweckmäßig $\alpha|2->$ und $\beta|2->$ für Spin "up" und "down")

(2 P)

4.) Gerechnen Sie für den in Ü3 gefundenen neuen Grundzustand die anisotropen g-Faktoren g$_z$, g$_x$=g$_Y$ durch "Einschalten" der Zeeman Ww: $\mu_B(\mathbf{L}+g_e\mathbf{S})\mathbf{H}$ (3 P)

Orbital magnetism in second order perturbation theory

$$\mathcal{H}' = \mu_B \mathbf{H} \cdot \mathbf{L} + \lambda \mathbf{L} \cdot \mathbf{S}$$

$$g_{\parallel} - g_{\perp} = g_e \lambda (\Lambda_{\perp} - \Lambda_{\parallel})$$

anisotropic $\mu_L \leftrightarrow$ MAE

$$
\mathcal{H} = \sum_{i,j=1}^{3} [\beta g_e(\delta_{ij} - \overbrace{2\lambda\Lambda_{ij}}^{g_{exp}})S_iH_j - \lambda^2\Lambda_{ij}S_iS_j]
$$

$$ + \text{ diamagnetic terms in } H_iH_j \qquad (3\text{-}23)$$

where Λ_{ij} is defined in relation to states ($n > 0$) as

$$\Lambda_{ij} = \sum_{n \neq 0} \frac{(0|L_i|n)(n|L_j|0)}{E_n - E_0} \qquad (3\text{-}24)$$

$$< o|\mu_B\mathbf{H}\cdot\mathbf{L}|n > < n|\lambda\mathbf{L}\cdot\mathbf{S}|o >$$

$$< o|\lambda\mathbf{L}\cdot\mathbf{S}|n > < n|\lambda\mathbf{L}\cdot\mathbf{S}|o >$$

In the principal axis system of a crystal with axial symmetry, the $\underline{\Lambda}$ tensor is diagonal with $\Lambda_{zz} = \Lambda_{\parallel}$ and $\Lambda_{xx} = \Lambda_{yy} = \Lambda_{\perp}$. Under these conditions, $\mathcal{H}$ of (3-23) can be simplified, since

$$S_x^2 + S_y^2 = S(S + 1) - S_z^2$$

to give

$$\mathcal{H} = g_{\parallel}\beta H_zS_z + g_{\perp}\beta(H_xS_x + H_yS_y) + D[S_z^2 - \tfrac{1}{3}S(S + 1)] \qquad (3\text{-}25)$$

where

$$g_{\parallel} = g_e(1 - \lambda\Lambda_{\parallel})$$
$$g_{\perp} = g_e(1 - \lambda\Lambda_{\perp})$$
$$D = \lambda^2(\Lambda_{\perp} - \Lambda_{\parallel}) \qquad (3\text{-}26)$$

G.E. Pake, p.66

$$D = \frac{\lambda}{g_e}\Delta g$$

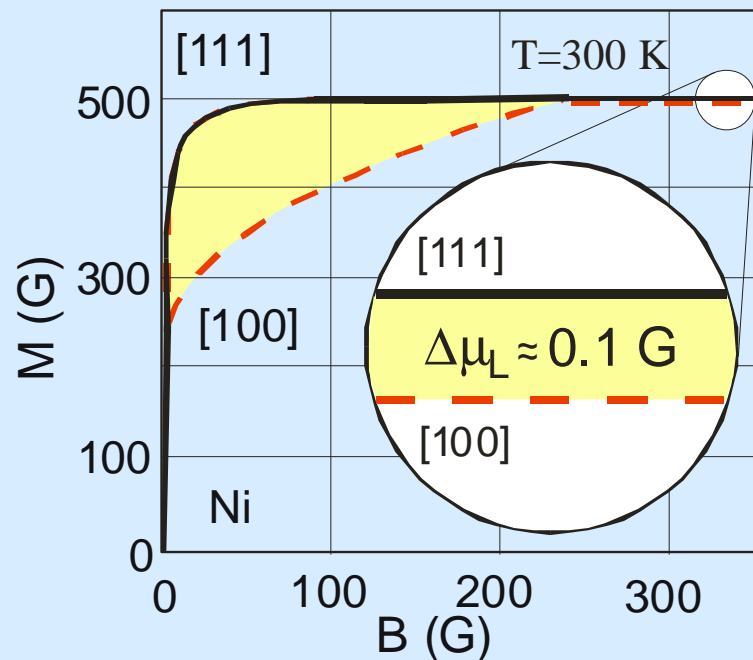$$\text{MAE} \propto \frac{\xi_{LS}}{4\mu_B}\Delta\mu_L$$

Bruno ('89)

Magnetic Anisotropy Energy (MAE)

1. Magnetic anisotropy energy = f(T)

2. Anisotropic magnetic moment ≠ f(T)

Characteristic energies of metallic ferromagnets

binding energy	1 - 10 eV/atom
exchange energy	$10 - 10^3$ meV/atom
cubic MAE (Ni)	0.2 µeV/atom
uniaxial MAE (Co)	70 µeV/atom

$$MAE = \int M \cdot dB \approx \frac{1}{2}\Delta M \cdot \Delta B \approx \frac{1}{2}200 \cdot 200 G^2$$

$$MAE \approx 2 \cdot 10^4 \, erg/cm^3 \approx 0.2\mu eV/atom$$

≈ 1µeV/atom is very small compared to
≈ 10 eV/atom total energy but all important

Spin reorientation in bulk Gd

THE TEMPERATURE DEPENDENCE OF THE ANISOTROPY COEFFICIENTS
from **B. COQBLIN**
p. 371
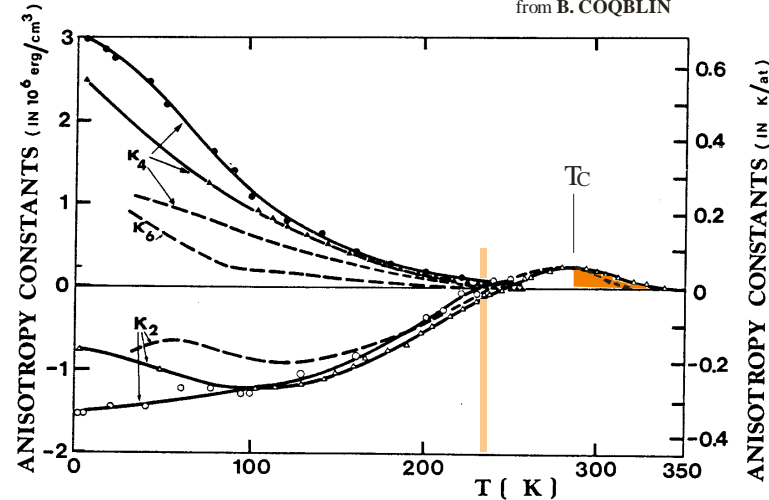
Fig. 160. Experimental values of the anisotropy constants κ_2, κ_4 and κ_6 versus temperature in Gadolinium. The circles (○ for κ_2, ● for κ_4) represent the data of Feron (Fig. 11 of Ref. 280), the triangles (△ for κ_2, ▲ for κ_4) the data of Graham (Fig. 1 of Ref. 66) and the full lines connect respectively the data of Feron and those of Graham. The dotted lines give the data of Corner *et al.* (Fig. 5 of Ref. 70 modified by Ref. 661) for κ_2, κ_4 and κ_6.

NIGH, LEGVOLD, AND SPEDDING PR **132**, 1092 (63)

Gd c AXIS
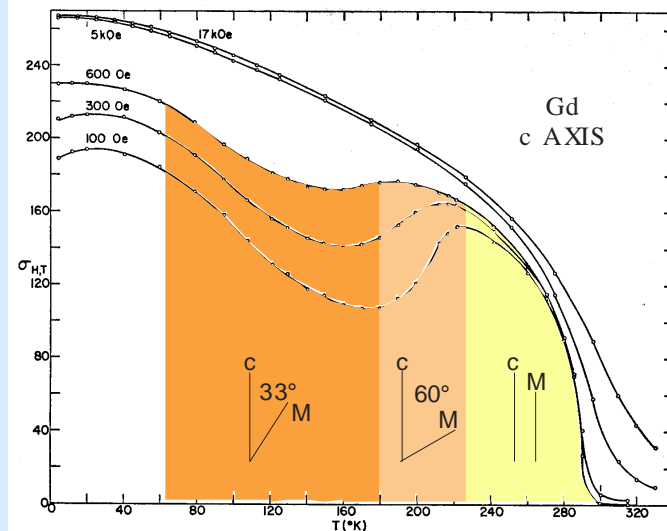
FIG. 4. Magnetic moment per gram versus temperature for the c-axis crystal. Internal magnetic fields are indicated.

Gd ist not isotropic, it has K_2, K_4, $K_6 \neq 0$

Note also finite MAE above T_C
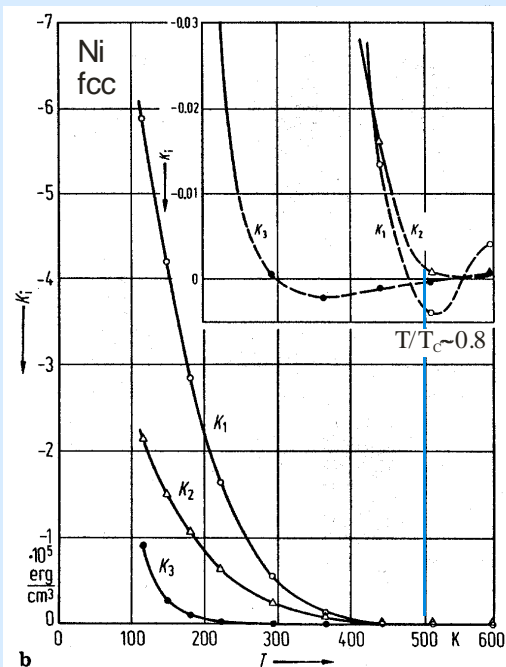
Spin reorientation in bulk Ni und Co

b

Fig. 7. Temperature dependence of magnetocrystalline anisotropy constants of Ni. (a) K_1. *1*: [68 F 1], *2*: [74 T 1], *3*: [77 B 2], *4*: [77 O 1]. Solid line: calculation [77 O 1]. (b) K_1, K_2, and K_3. Accuracy of data is considerably reduced near T_C: dashed lines in the insert [68 A 1]. (c) K_3. *1* and *2*: [76 A 1], *3*: [69 F 2], *4*: [77 B 2]. Solid line is to guide the eye through confidence limits [76 A 1].

FIG. 6. The variation of the initial susceptibility with temperature in nickel.

SRT for hcp Co
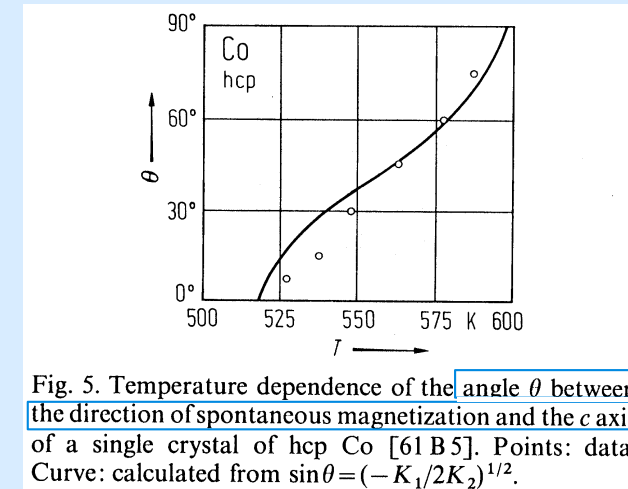$$\sin\theta = (K_2/2K_4)^{1/2}$$

Fig. 5. Temperature dependence of the angle θ between the direction of spontaneous magnetization and the c axis of a single crystal of hcp Co [61 B 5]. Points: data. Curve: calculated from $\sin\theta = (-K_1/2K_2)^{1/2}$.

LB III, 19a, p.45

At the extremal value of K_2 a reorientation and second maximum in χ appears

Superstarke Magnete intermetallischer Verbindungen der Seltenerdmetalle

Leistungssteigerung durch nanokristalline Strukturen

H. Kronmüller
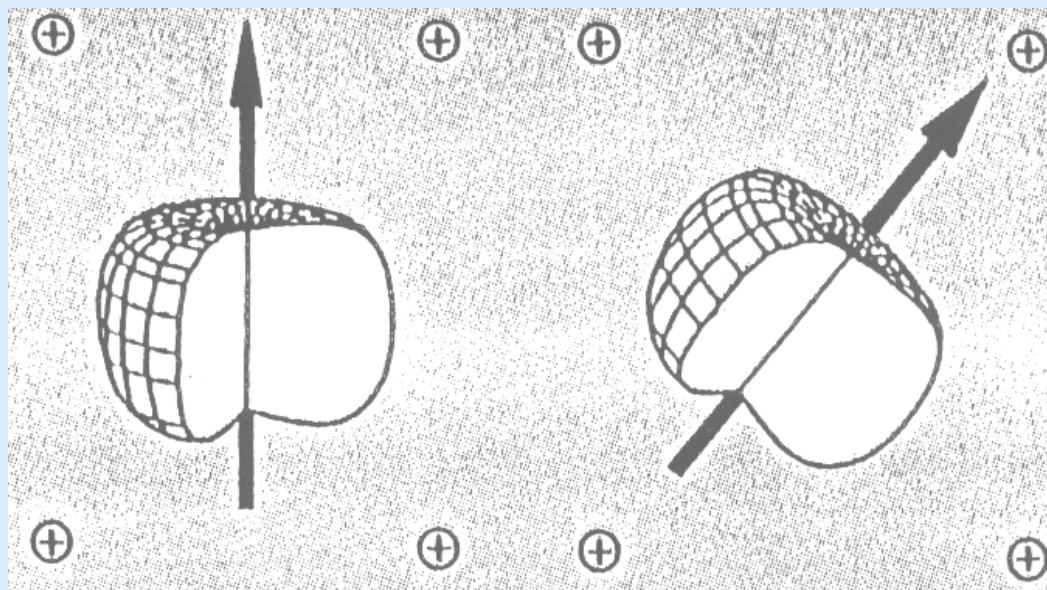
Abb. 3: **Die Vorzugsrichtung des magnetischen Moments** (*leichte Richtung*) der intermetallischen Seltenerdverbindungen **hat ihre Ursache in** der starren Kopplung zwischen **magnetischem Moment** (Pfeil) **und Ladungsverteilung** der 4f-Eletronen des Neodym. Bei einer Rotation des magnetischen Moments aus der c-Richtung (senkrecht) heraus dreht sich die anisotrope Ladungswolke mit. Da die Wechselwirkungsenergie zwischen 4f-Ladungswolke und Ladungswolken der benachbarten Ionen (⊕) dabei zunimmt, wird die leichte Richtung favorisiert.

Free energy density of MAE, K

(intrinsic, after substraction of $2\pi M^2$)

tetragonal [e.g. Ni, Co, Fe (001) / Cu (001)]:

$E_{tetr} = - K_2 \alpha_z^2 \qquad\qquad - \tfrac{1}{2} K_{4\perp} \alpha_z^4 - \tfrac{1}{2} K_{4\|}(\alpha_x^4 + \alpha_y^4) + ... \qquad$ *(B.Heinrich et al.)*

$\quad = - K_2 \cos^2\theta \qquad\qquad - \tfrac{1}{2} K_{4\perp} \cos^4\theta - \tfrac{1}{2} K_{4\|} \tfrac{1}{4} (3+\cos 4\varphi) \sin^4\theta + ... \quad$ *(Bab et al.)*

$\quad = (K_2 + K_{4\perp}) \sin^2\theta \qquad - \tfrac{1}{2} (K_{4\perp} + \tfrac{3}{4} K_{4\|}) \sin^4\theta - \tfrac{1}{8} K_{4\|} \cos 4\varphi \sin^4\theta + ...$

$\quad = K_2' \sin^2\theta \qquad\qquad + K_{4\perp} \sin^4\theta + K_{4\|} \cos 4\varphi \sin^4\theta + ... \qquad$ *(traditional)*

hexagonal [e.g. Ni (111), Gd (0001) / W (110)]:

$E_{hex} = k_2 \sin^2\theta + \tfrac{1}{2} k_{2\|} \cos 2\varphi \sin^2\theta + k_4 \sin^4\theta + k_{6\perp} \sin^6\theta + k_{6\|} \cos 6\varphi \sin^6\theta + ...$

$K = k_2 Y_2^0 + k_{4m} Y_4^m + ... \qquad$ *Legendre polyn. (B. Coqblin)*

each K_i has a „volume" and „surface" contribution
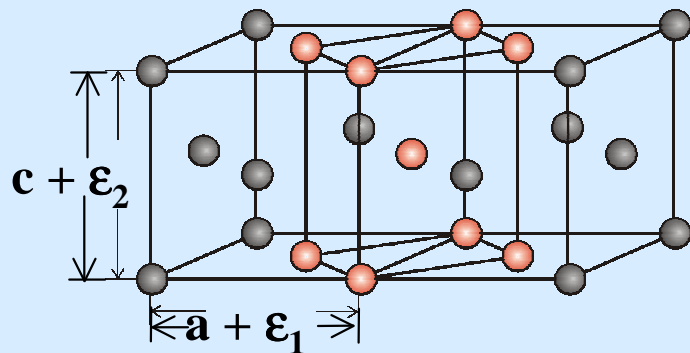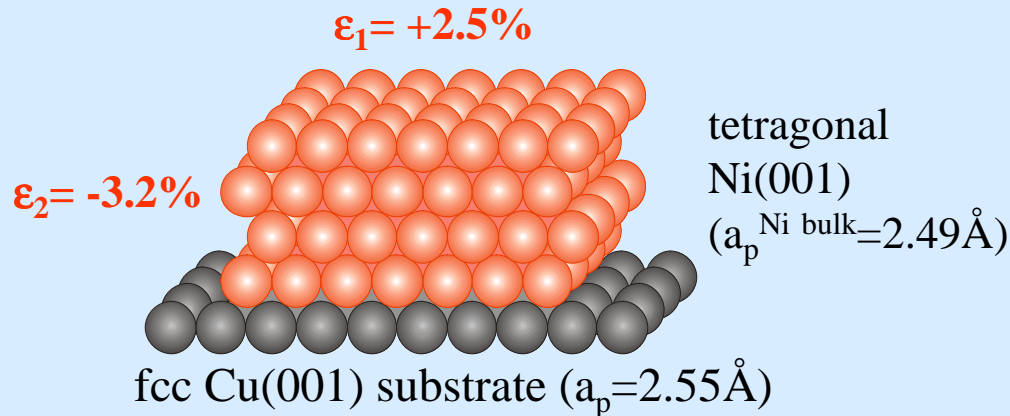
$$K_i = K_i^v + 2K_i^s/d$$
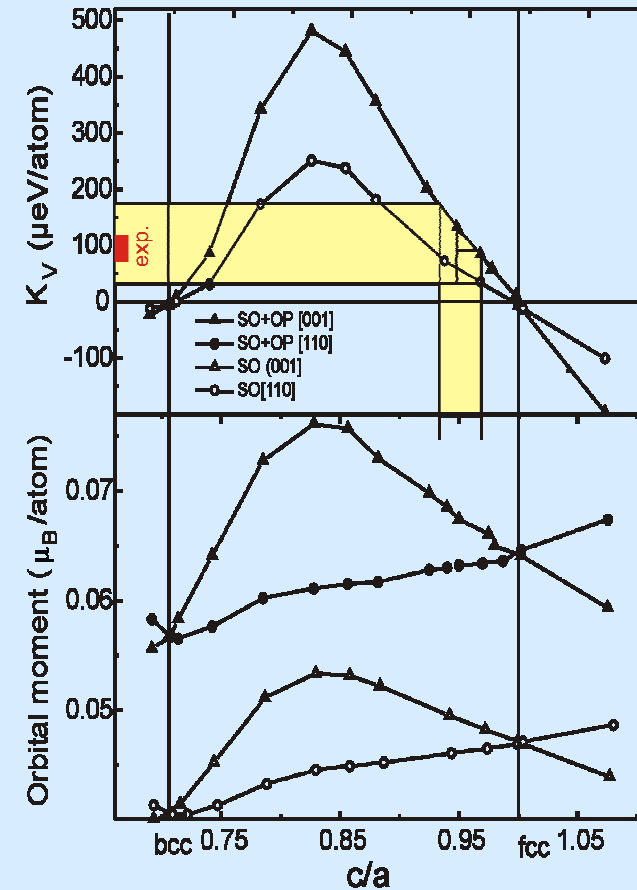
2. Magnetic Anisotropy Energy (MAE) in ultra thin films

There are <u>only 2 origins</u> for MAE: 1) dipol-dipol interaction $\sim (\bar{\mu}_1 \bullet \bar{r})(\bar{\mu}_2 \bullet \bar{r})$ and
2) spin-orbit coupling $\lambda \bar{L} \bar{S}$ (intrinsic K or ΔE_{band})

Growth of artificial nanostructures
bcc, fcc $\rightarrow$ tetragonal, trigonal

$\varepsilon_1 = +2.5\%$

$\varepsilon_2 = -3.2\%$

tetragonal
Ni(001)
($a_p^{Ni\ bulk} = 2.49$Å)

fcc Cu(001) substrate ($a_p = 2.55$Å)

$c + \varepsilon_2$

$\overline{a} + \varepsilon_1$

Bain path

$c/a = 1$ fcc $\rightarrow$ fct $\rightarrow$ bcc $c/a = 1/\sqrt{2}$

Structural changes by ≈ 0.05 Å increase MAE by 2-3 orders of magnitude ($\sim 0.2 \rightarrow 100 \mu$eV/atom)

O. Hjortstam, K. B. et al. PRB **55**, 15026 ('97)
R. Wu et al. JMMM **170**, 103 ('97)

FMR in ferromagnetic nanostructure

In situ UHV-FMR set up
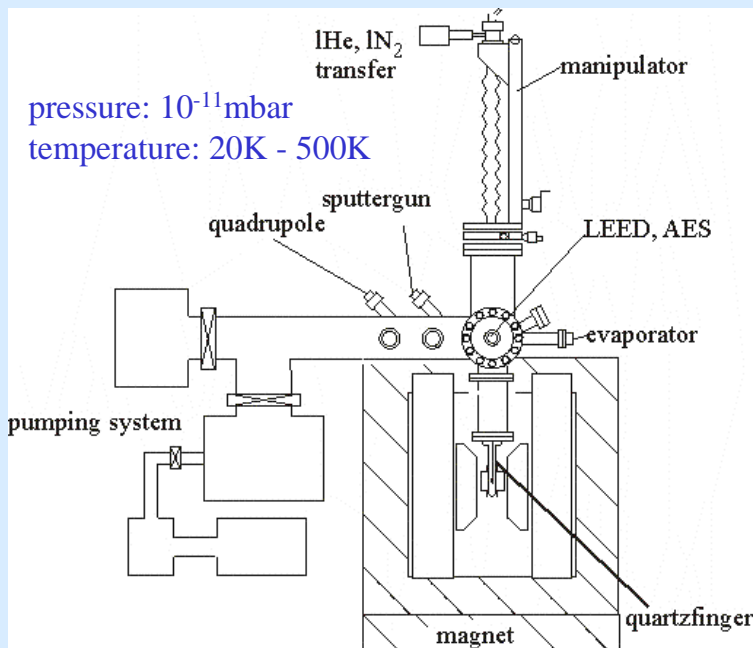
pressure: 10^{-11} mbar
temperature: 20K - 500K

lHe, lN₂ transfer — manipulator
sputtergun
quadrupole
LEED, AES
evaporator
pumping system
quartzfinger
magnet

lHe cryostat
thermocouple
cavity
sample
UHV
quartzfinger
electromagnet
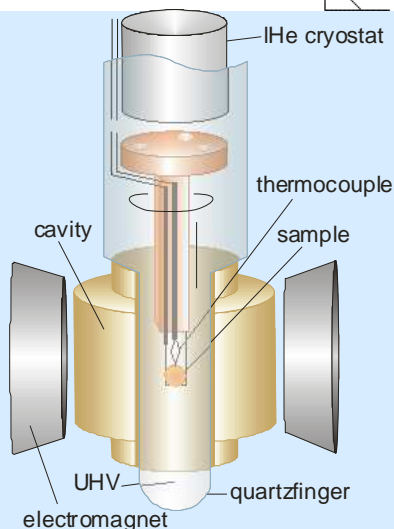
M. Zomak et al.,
Surf. Sci. **178**, 618 (1986)

J. Lindner, K.B.
J. Phys.: Cond. Matt **15**, R193 (2003)
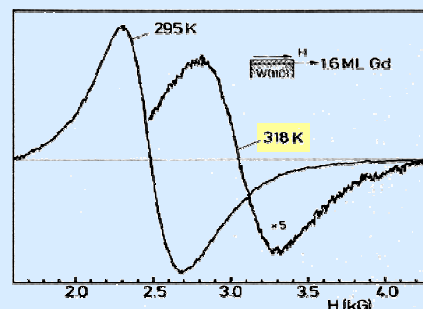
Fig. 4. ESR spectra for the new 1.6 ML sample (not cited in [2, 3]). Note the significant change in intensity and resonance field from 16 to 39 K above T_c.
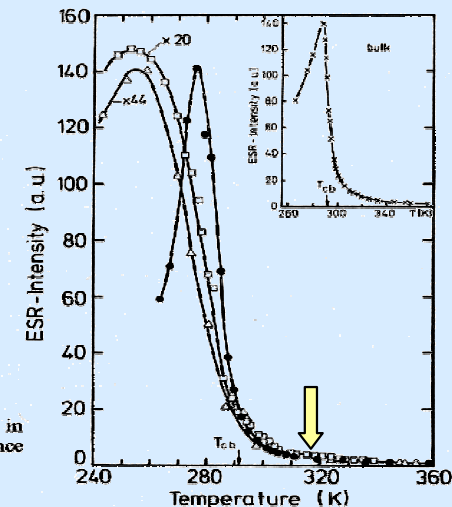
Fig. 5. Area of the ESR signal as a function of temperature for 80 Å (●), the new 1.6 ML (□), and the 0.8 ML (△). The insert shows the same data for a 18 μm thick Gd foil (bulk). Solid lines are guides to the eye. The 1.6 and 0.8 ML have a vertical gain factor of 20 and 44 with respect to 80 Å. The insert is not to scale
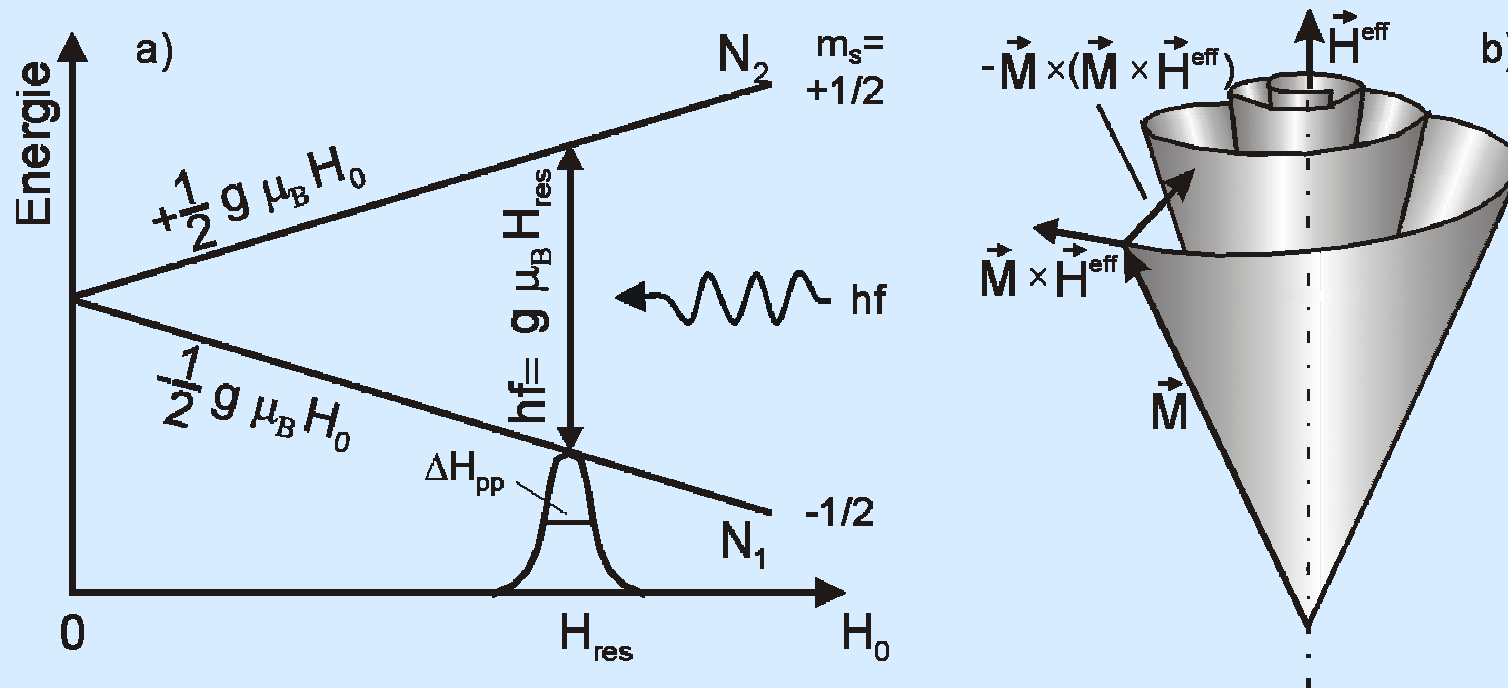

7.2 ML Ni/Cu(001)
T=297 K
3.97 GHz
9.00 GHz
1.12 GHz
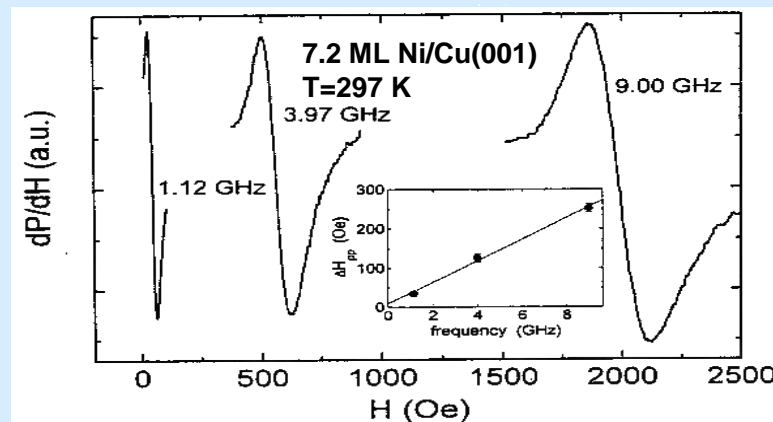
W. Platow,
Ph.D. thesis
(1999)

Magnetic resonance (ESR, FMR)

Landau-Lifshitz-Gilbert-Equation

$$\frac{1}{\gamma}\frac{\partial M}{\partial t} = -(M \times H_{eff}) + \frac{G}{\gamma^2 M_S^2}\left(M \times \frac{\partial M}{\partial t}\right)$$
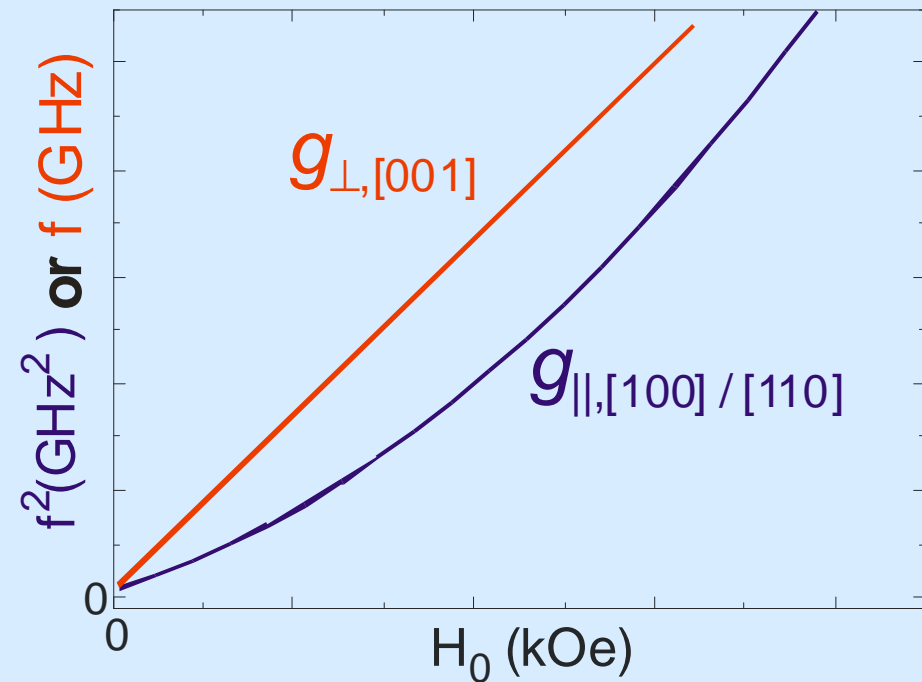
Determination of g-Tensor components

$$\frac{\omega^2}{\gamma^2_{\parallel,[100]}} = H^2_{0,[100]} + H_{0,[100]}\left(4\pi M - 2\frac{K_2}{M} + \frac{4K_{4\parallel}}{M}\right) + 2\frac{K_{4\parallel}}{M}\left(4\pi M - 2\frac{K_2}{M} + \frac{2K_{4\parallel}}{M}\right)$$

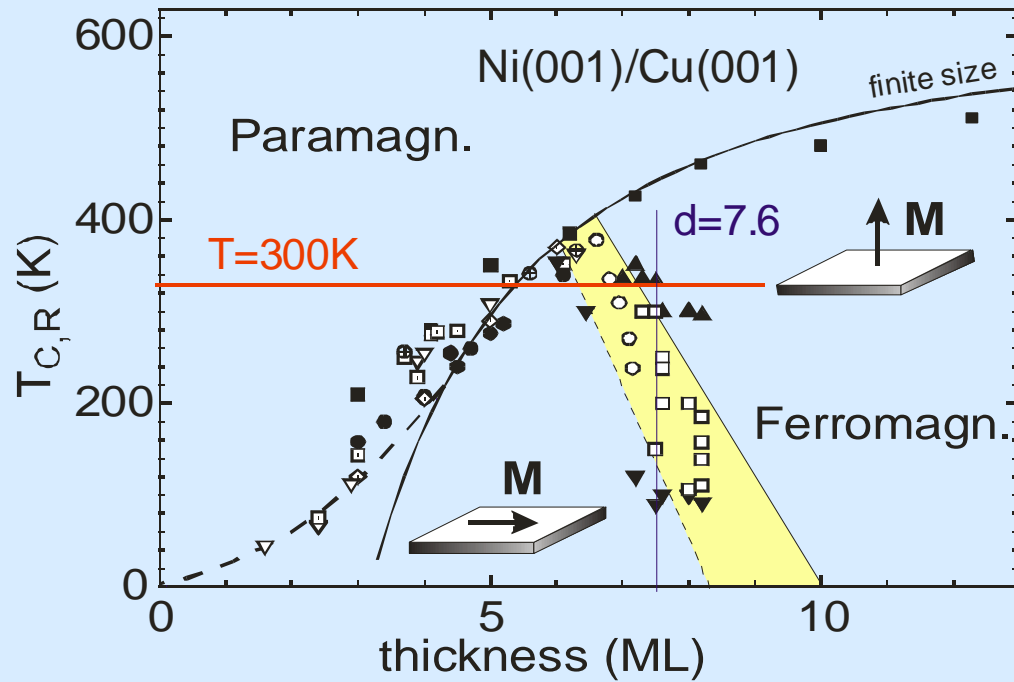$$\frac{\omega}{\gamma_{\perp,[001]}} = H_{0,\perp} - 4\pi M + \frac{2(K_2 + K_{4\perp})}{M}$$

with $\gamma = \dfrac{g \cdot \mu_B}{\hbar}$
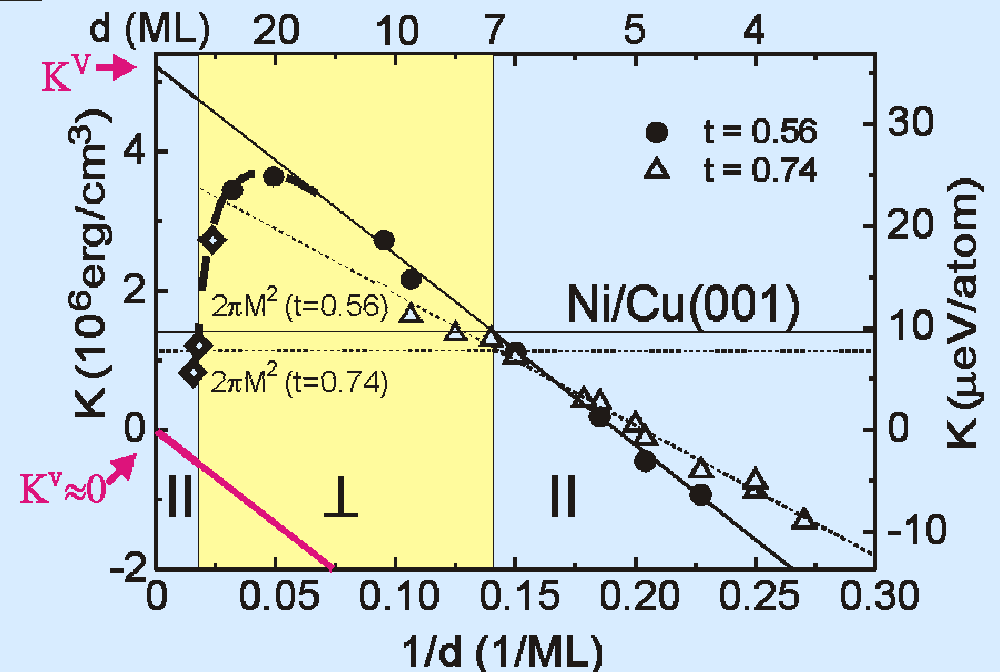
$$\frac{\mu_l}{\mu_s} = \frac{g-2}{2}$$
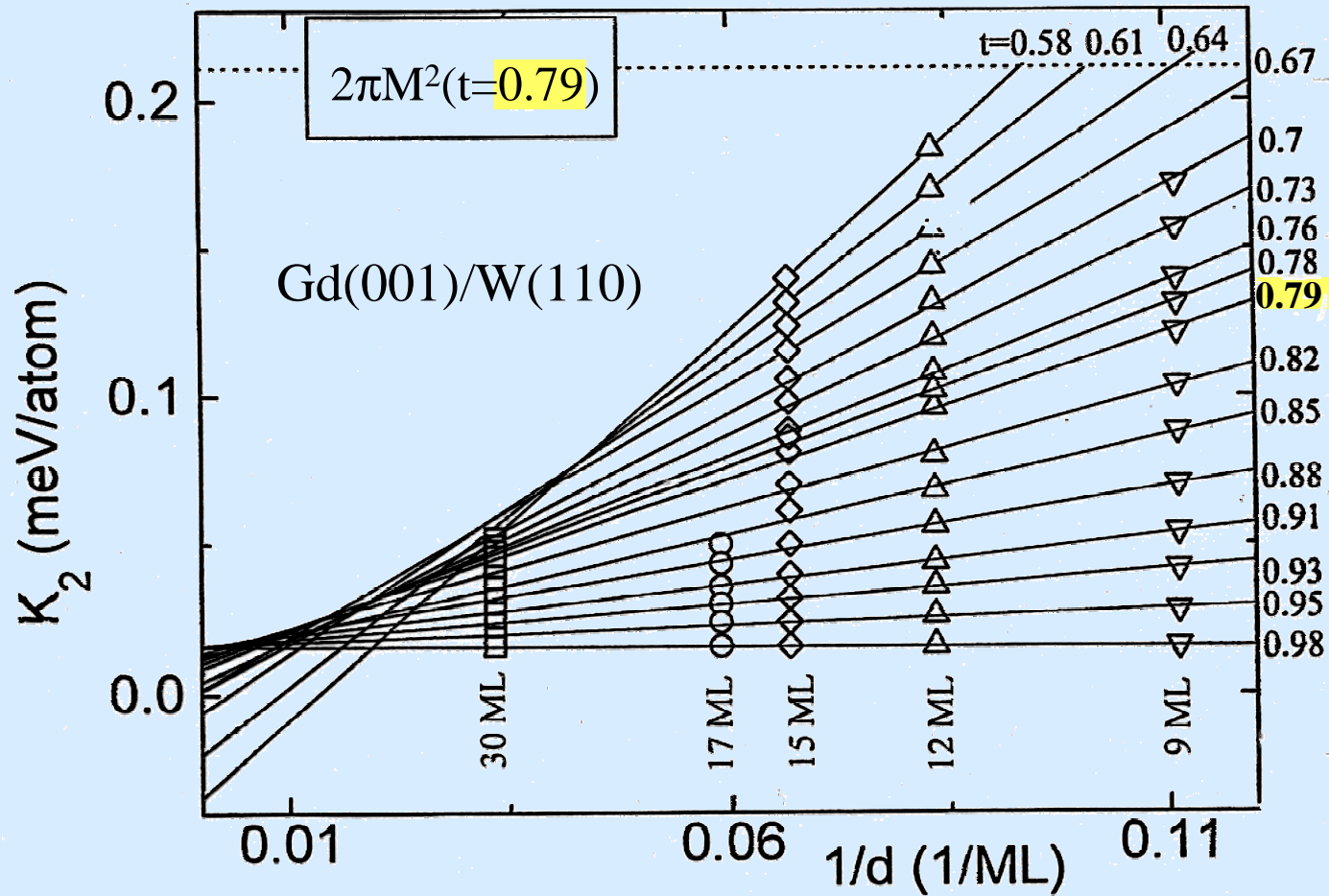
C. Kittel, *J.Phys. Radiat.* **12**, 291 (1951)

For thin films the Curie temperature can be manipulated

Ni(001)/Cu(001)

Paramagn.

T=300K

d=7.6

M

M

Ferromagn.

finite size

$T_{C,R}$ (K)

thickness (ML)
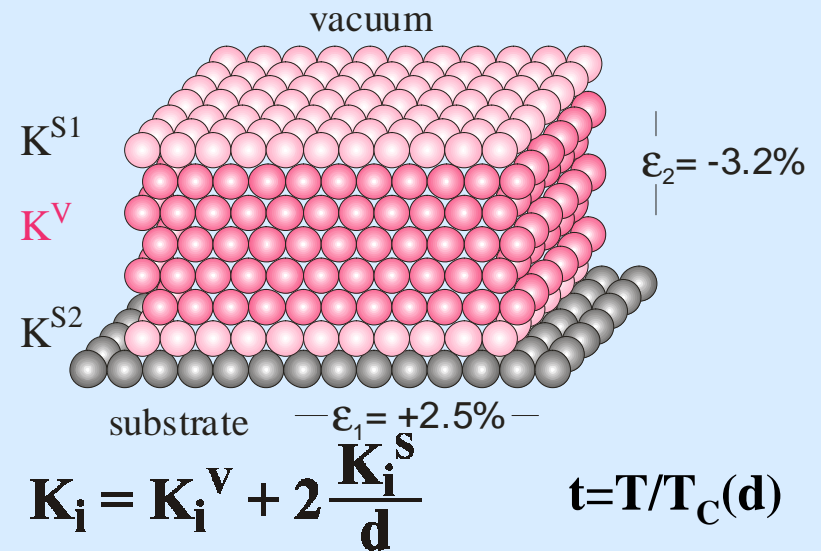
P. Poulopoulos and K. B.
J. Phys.: Condens. Matter **11**, 9495 (1999)

vacuum

K^{S1}

K^{V}

K^{S2}

substrate

$\varepsilon_2 = -3.2\%$

$\varepsilon_1 = +2.5\%$

$$K_i = K_i^V + 2\frac{K_i^S}{d} \qquad t=T/T_C(d)$$

d (ML)   20   10   7   5   4

K^V

$K^v \approx 0$

$2\pi M^2$ (t=0.56)

$2\pi M^2$ (t=0.74)

Ni/Cu(001)

- t = 0.56
△ t = 0.74

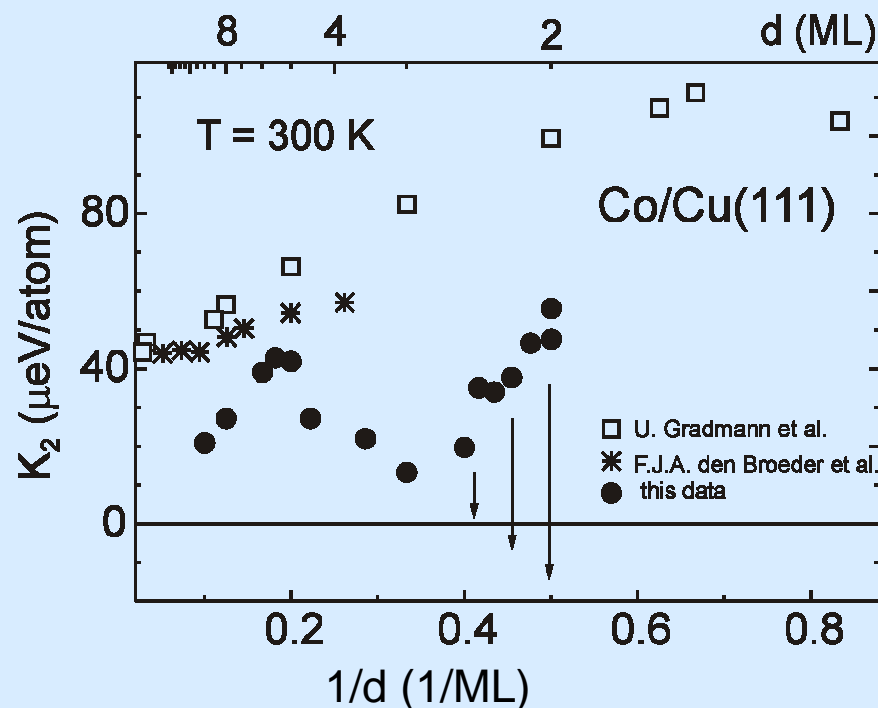‖   ⊥   ‖

K (10^6erg/cm^3)

K (µeV/atom)

1/d (1/ML)

G. André et al., Surface Science **326**, 275 (1995)
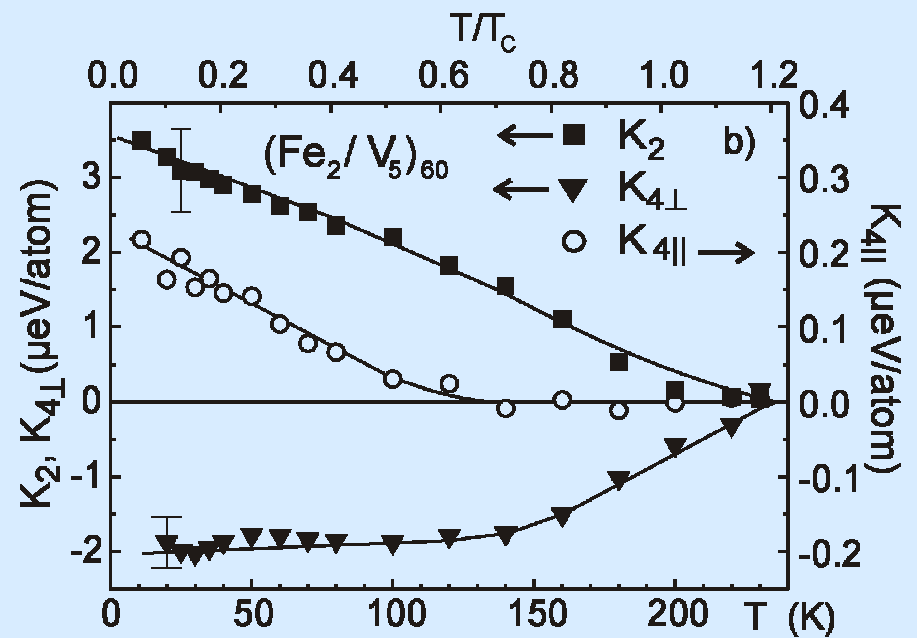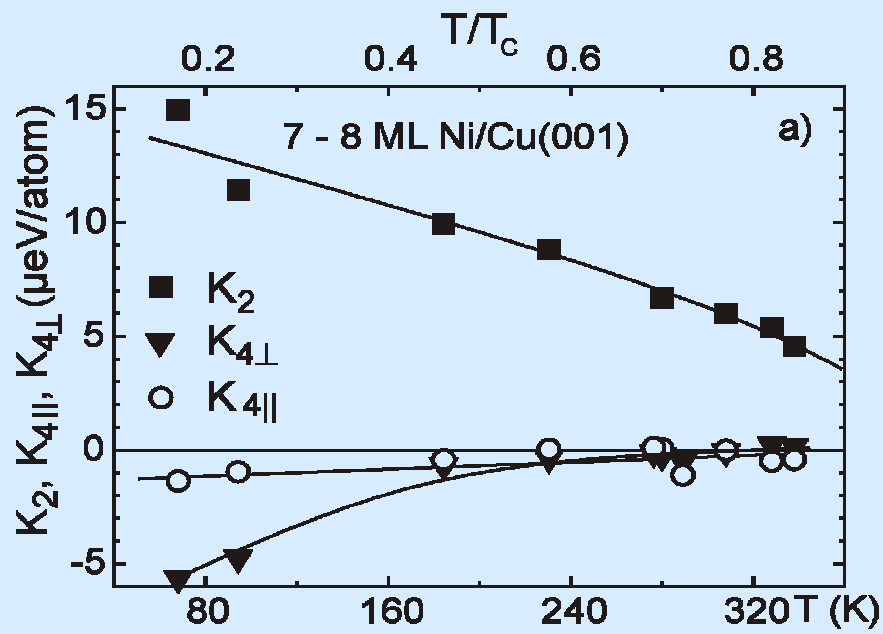K. Baberschke and M. Farle, J. Appl. Phys. **81**, 5038 (1997)
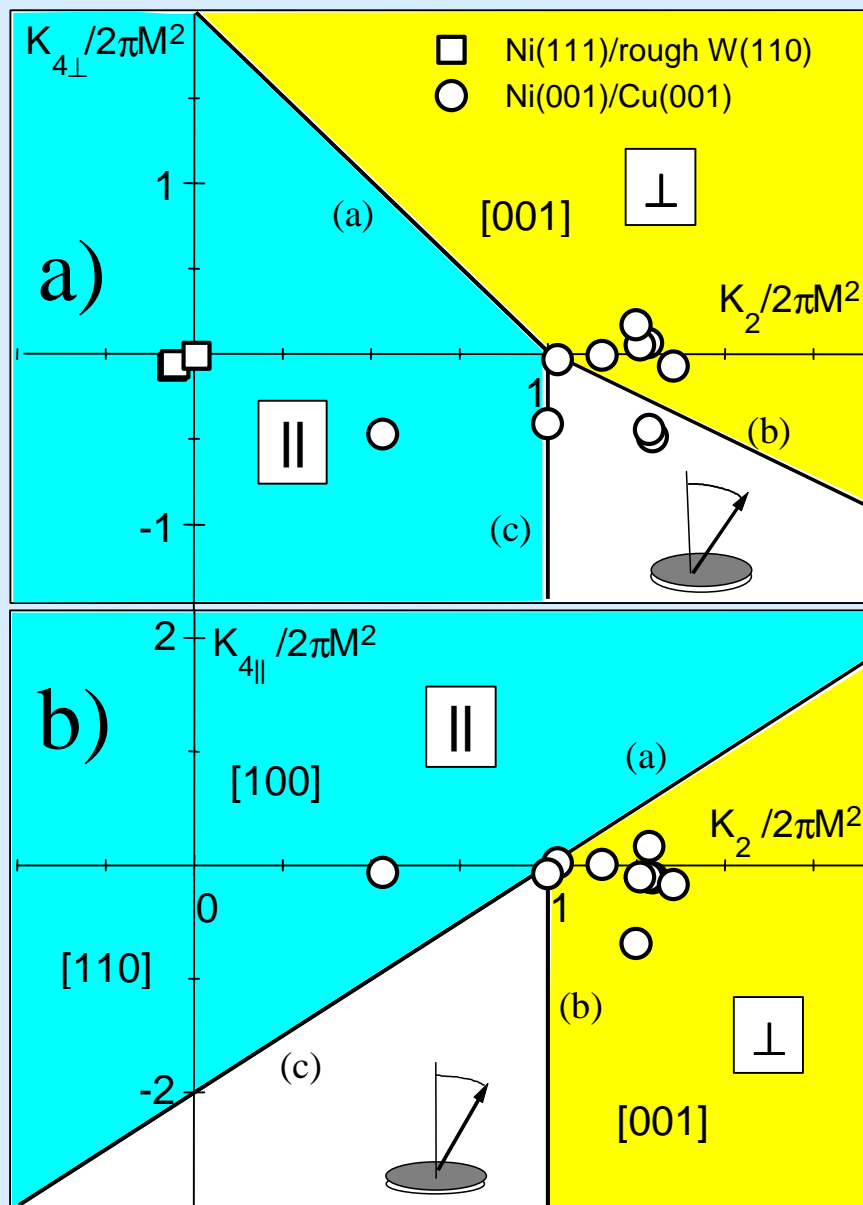
K is temperature dependent $\Rightarrow$ K (T/T$_C$)
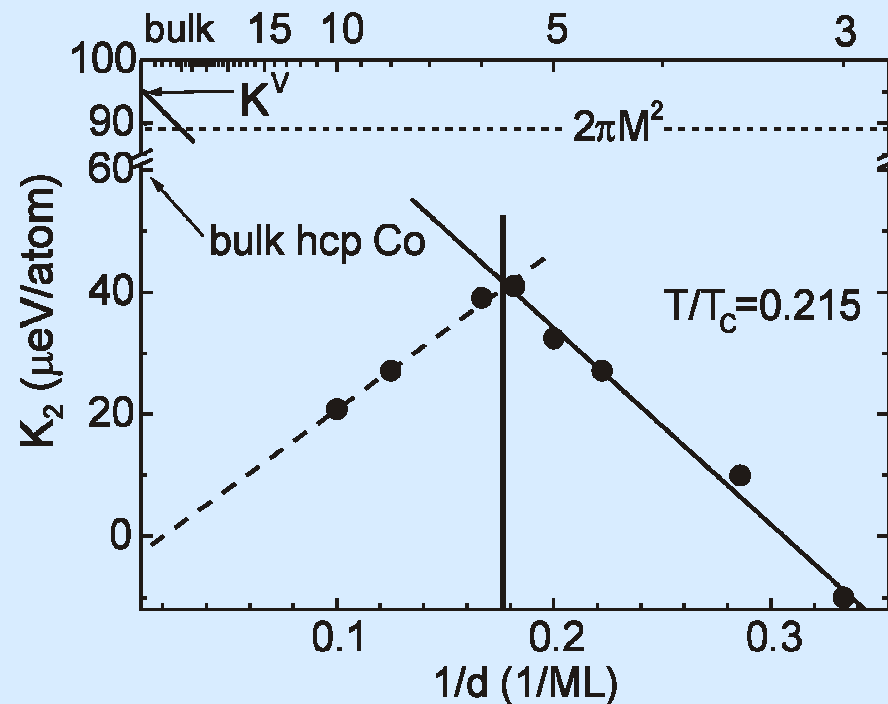
M. Farle et al., Surf. Sci. **439**, 146 (1999)

If d changes also T$_C$(d) shifts
taking this into consideration we found for all systems a 1/d dependence

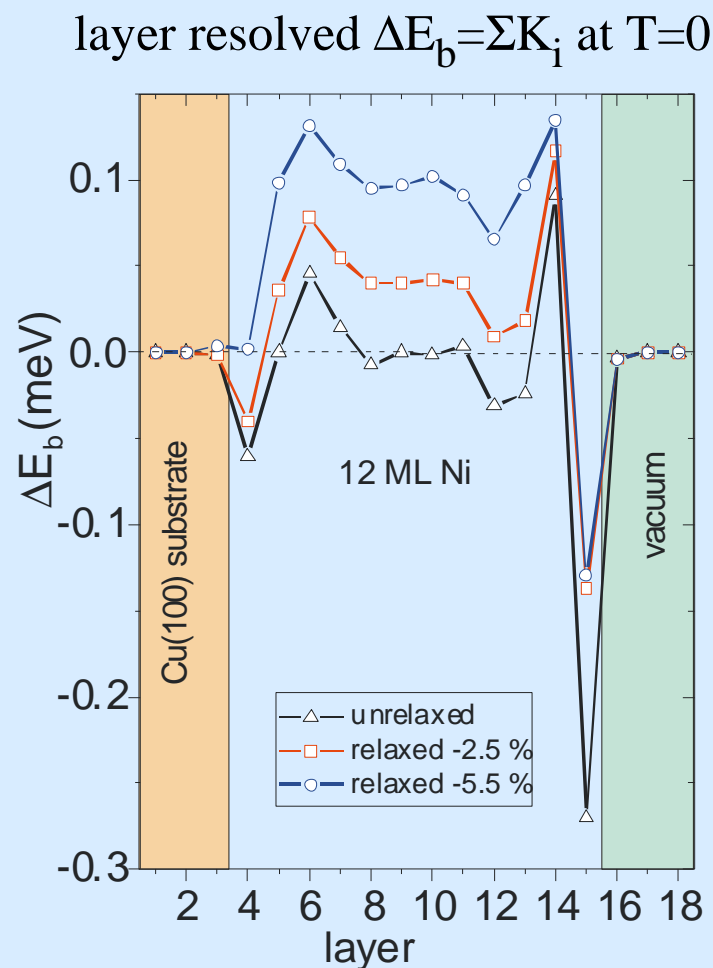A. Berghaus, M. Farle, Yi Li, K. Baberschke
Absolute determ. of the mag. anisotropy of ultrathin Gd and Ni/W(110).
Second Intern. Workshop on the Magnetic Properties of Low-Dimensional Systems.
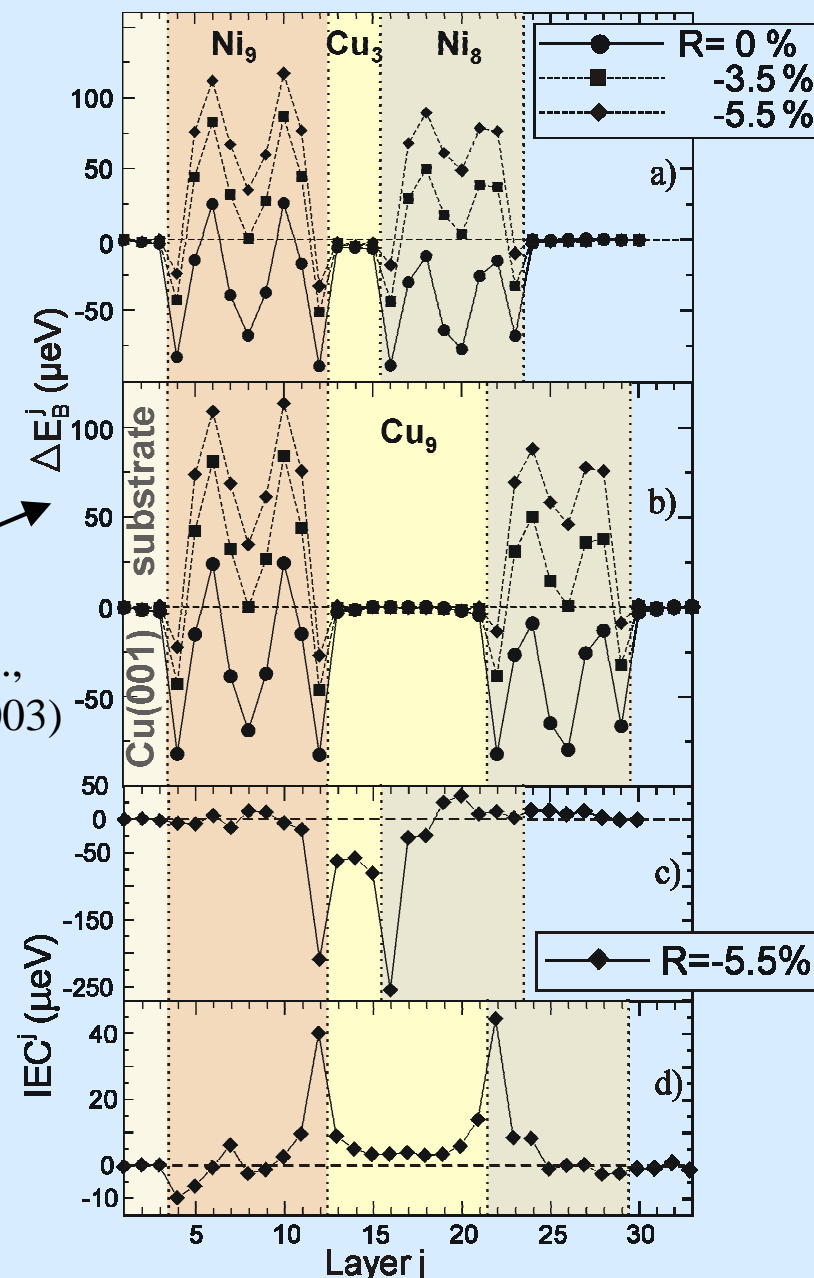San Luis Potosi, Mexico, Proc. in Physics **50**, 61 (1989)

M. Farle et al., PRB **55**, 3708 (1997)

SP-KKR calculation for rigit fcc and relaxed fct structures

layer resolved $\Delta E_b = \Sigma K_i$ at T=0

C. Uiberacker et al., PRL **82**, 1289 (1999)

R. Hammerling et al., PRB **68**, 092406 (2003)

The surface and interface MAE are certainly large (L. Néel, 1954) but count only for one layer each. The inner part (volume) of a nano-structure will overcome this, because they count for n-2 layers.

Summary of Chap. 2

- Historical names like „crystalline" or „magnetoelastic" anisotropy energy should not be used in nanostructures. It is all SO interaction, or better, a fully relativistic treatment (full potential, etc.).

- Atoms at edges, steps have different K-values.

- Small changes in the local structure ~ few/100 Å may change the MAE dramatically.

- In most cases K depends on the reduced temperature $t=T/T_C(d)$.

- The experiments measure in most cases the sum of dipole and intrinsic (bandstructure) K.

- The dipole term may not be $2\pi M^2$ (see PhD thesis, Farle 1989).

3. Orbital magnetic moment μ_L

Which technique measures what?
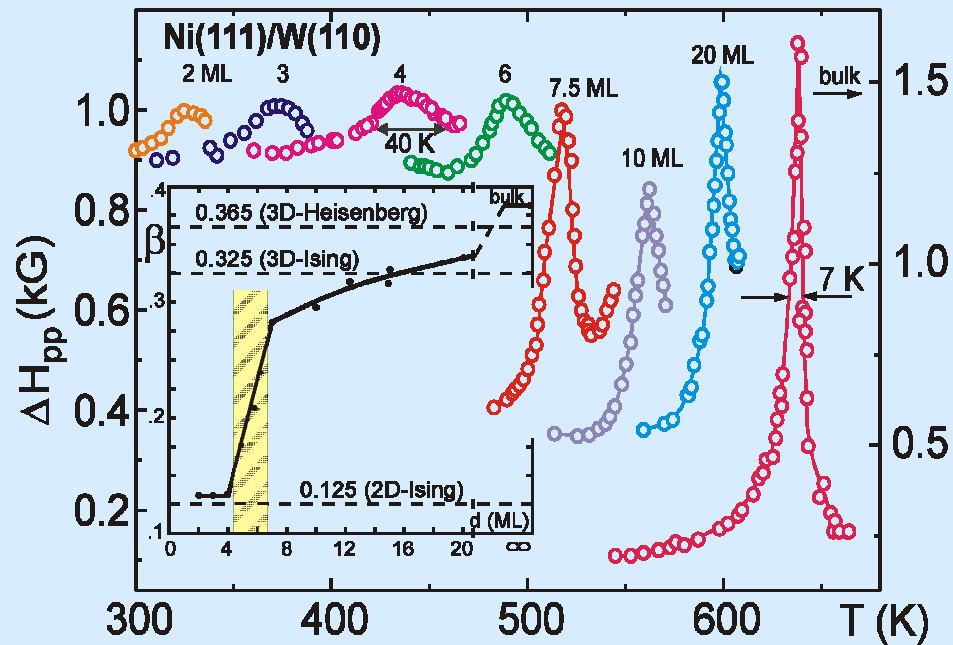
μ_L / μ_S in UHV-FMR

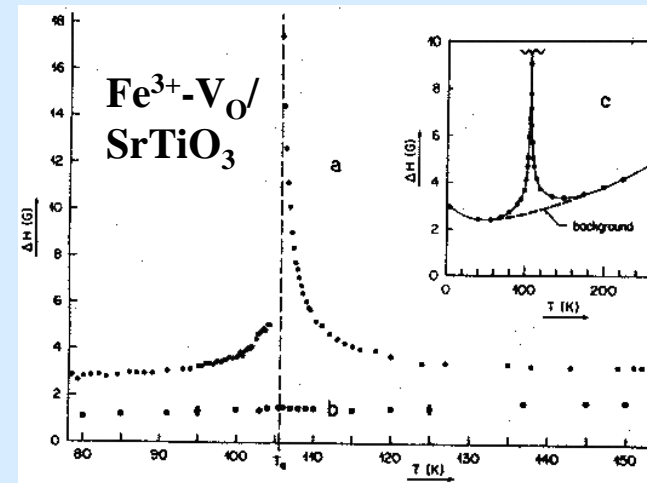μ_L , μ_S in UHV-XMCD

$\mu_L + \mu_S$ in UHV-SQUID

per definition:

1) spin moments are isotropic

2) also exchange coupling $\mathbf{J}\, \mathbf{S_1 \cdot S_2}$ is isotropic

3) so called anisotropic exchange is a (hidden) projection of the orbital momentum onto spin space

FMR/ESR line witdth at the phase transition

Yi Li, K. B., PRL **68**, 1208 (1992)

Th.v. Waldkirch, K.A. Müller, W. Berlinger, PRB (1973)

R.P. Erickson & D.L. Mills PRB **44**, 11825 (91)

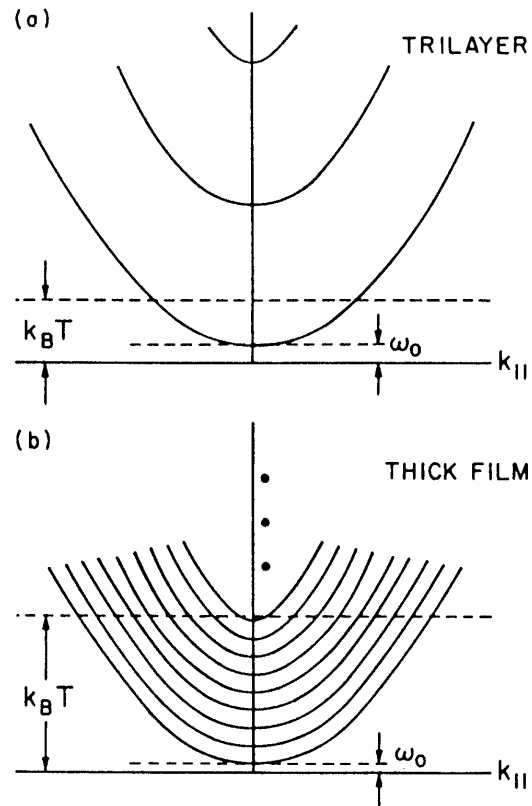FIG. 4. Depicted are (a) the spin-wave normal modes of a trilayer, sketched at room temperature, and (b) the spin-wave "minibands" in a thick layer.

Spin wave branches $= \omega_0 + \dfrac{1}{2}D\{k_{II}^2 + [\dfrac{\pi}{Nd}]^2\}$

d: spacing
N: layers
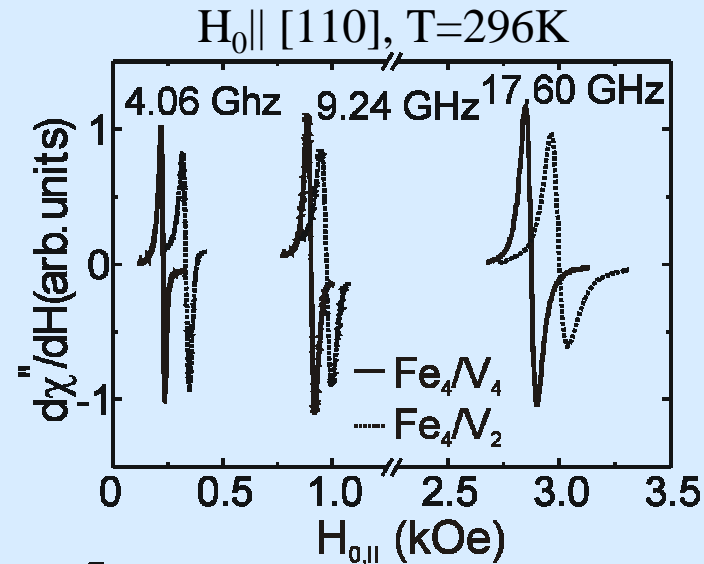
"A criterion for a crossover from quasi 2D to 3D is…"

$$N_C = \sqrt{\dfrac{\hbar D}{kT}} \cdot \dfrac{\pi}{d}$$
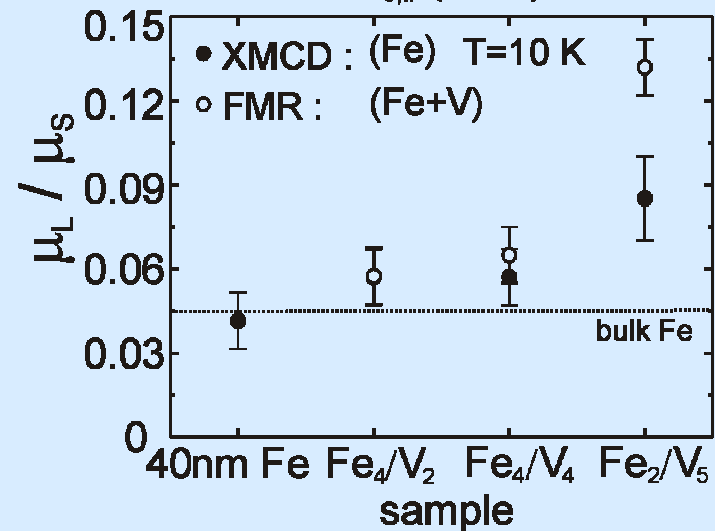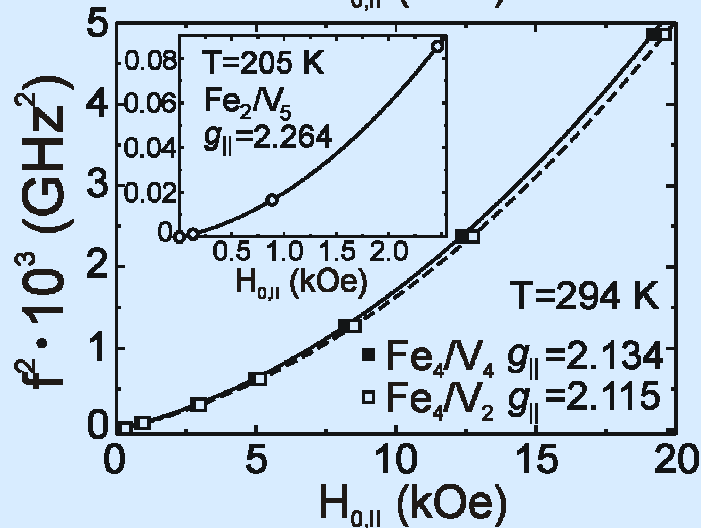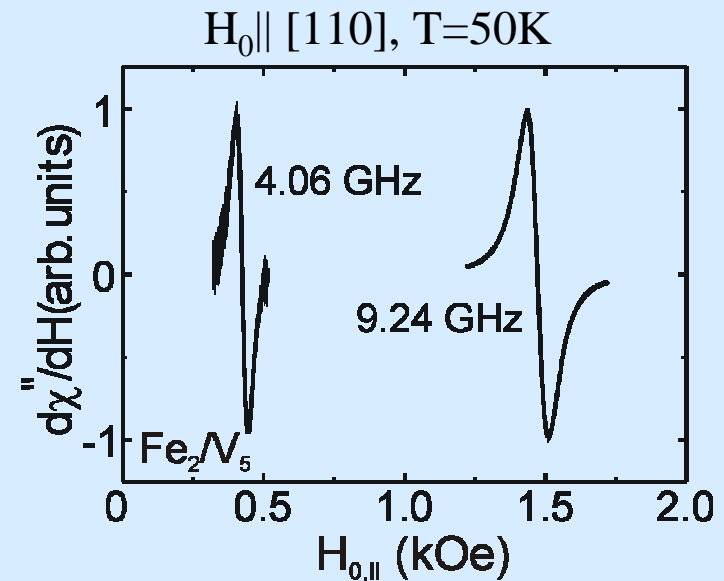
D: stiffness const.

Ni: $\hbar D \approx 4 \cdot 10^{-1}\,\mathrm{eV\,\AA^2}$;   d$= 2.03\,\AA$

$T = 300 \sim 500\,\mathrm{K} \Rightarrow N_C \approx 6 - 5$ layers

FMR in Fe_n/V_m superlattices

$H_0\|$ [110], T=296K

4.06 Ghz   9.24 GHz   17.60 GHz

$d\chi''/dH$(arb. units)

— Fe_4/V_4
---- Fe_4/V_2

$H_{0,\|}$ (kOe)

$g_{\|,[110]}$

$H_0\|$ [110], T=50K

4.06 GHz

9.24 GHz

Fe_2/V_5

$d\chi''/dH$(arb. units)

$H_{0,\|}$ (kOe)

$f^2 \cdot 10^3$ (GHz^2)

T=205 K
Fe_2/V_5
$g_\| = 2.264$

$H_{0,\|}$ (kOe)

T=294 K
■ Fe_4/V_4 $g_\| = 2.134$
□ Fe_4/V_2 $g_\| = 2.115$

$H_{0,\|}$ (kOe)

μ_L / μ_S

● XMCD : (Fe)   T=10 K
○ FMR :   (Fe+V)

bulk Fe

40nm Fe Fe_4/V_2 Fe_4/V_4 Fe_2/V_5
sample
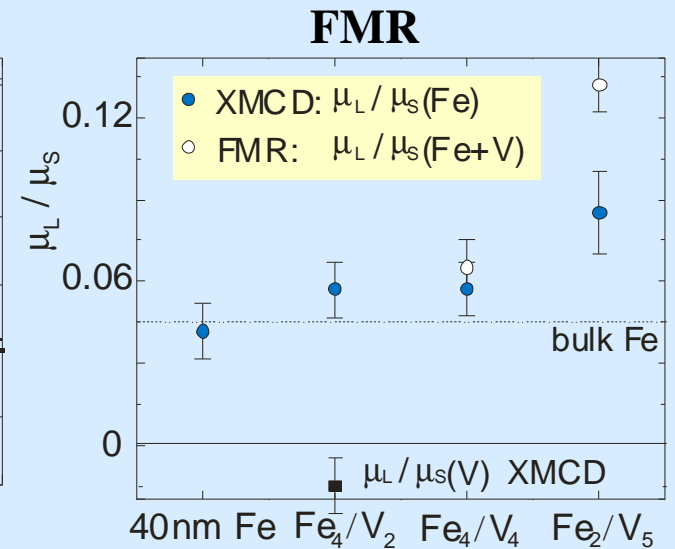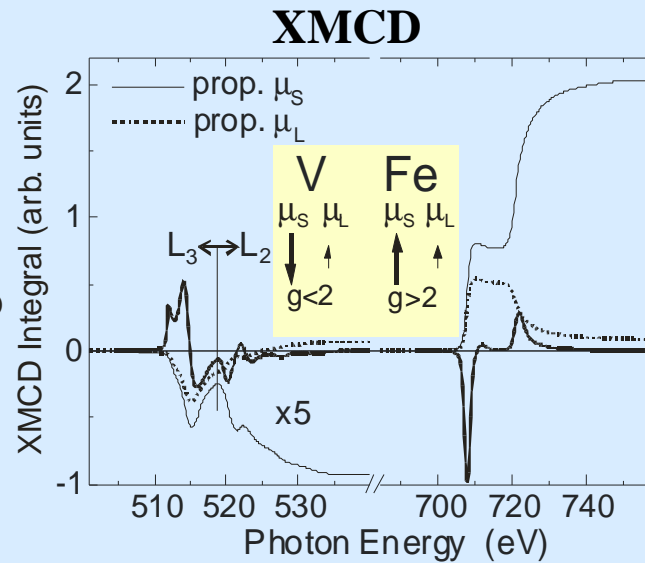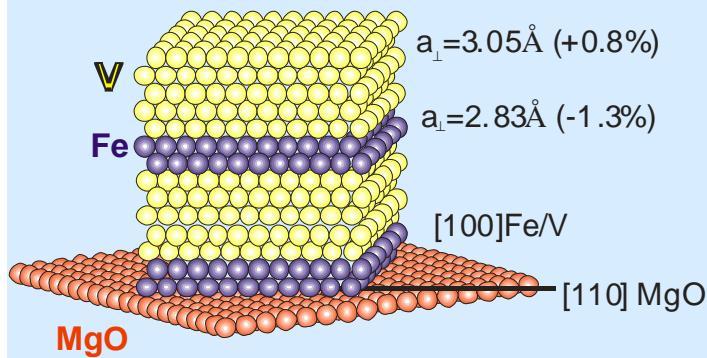
A.N. Anisimov et al., Phys. Rev. Lett. **82**, 2390 (1999)
A. Scherz et al., Phys. Rev. B **64**, 180407(R) (2001)

Ferromagnetic resonance on $Fe_n/V_m(001)$ superlattices

$a_\perp = 3.05$Å (+0.8%)

V

$a_\perp = 2.83$Å (-1.3%)

Fe

[100] Fe/V

[110] MgO

MgO

XMCD

XMCD Integral (arb. units)

— prop. μ_S
···· prop. μ_L

V   Fe
μ_S μ_L μ_S μ_L

$L_3 \leftrightarrow L_2$

g<2   g>2

x5

Photon Energy (eV)

510 520 530   700 720 740

FMR

μ_L / μ_S

● XMCD: μ_L / μ_S (Fe)
○ FMR: μ_L / μ_S (Fe+V)

bulk Fe

μ_L / μ_S (V) XMCD

40nm Fe Fe_4/V_2 Fe_4/V_4 Fe_2/V_5

$$\frac{\mu_L}{\mu_S} = \frac{g-2}{2}$$ (Kittel'49)

In solids g and μ_L are tensors

a)

T/T_C

0.0 0.2 0.4 0.6 0.8 1.0 1.2

$K_2, K_{4\perp}$ (µeV/atom)

$K_{4\parallel}$ (µeV/atom)

← ○ K_2
← ◇ $K_{4\perp}$
□ $K_{4\parallel}$ →

b)

MAE (µeV/atom)

MAE = $E_{[001]} - E_{[110]}$

Fe_2V_5

T (K)

0   50   100   150   200

A.N. Anisimov et al.
J. Phys. C **9**, 10581 (1997)
and PRL **82**, 2390 (1999)
and Europhys. Lett. **49**, 658 (2000)

bcc (001) Fe_2/V_5 superlattice					
$g_\parallel$	$g_\perp$	μ_L/μ_S	$\mu_L (\mu_B)$	$\mu_S (\mu_B)$	MAE µeV/atom
2.264	2.268	0.133	0.215	1.62	-2.0
bcc Fe-bulk					
2.09	2.09	0.045	0.10	2.13	-1.4

$L_{3,2}$ XAS and XMCD of *3d* TM's
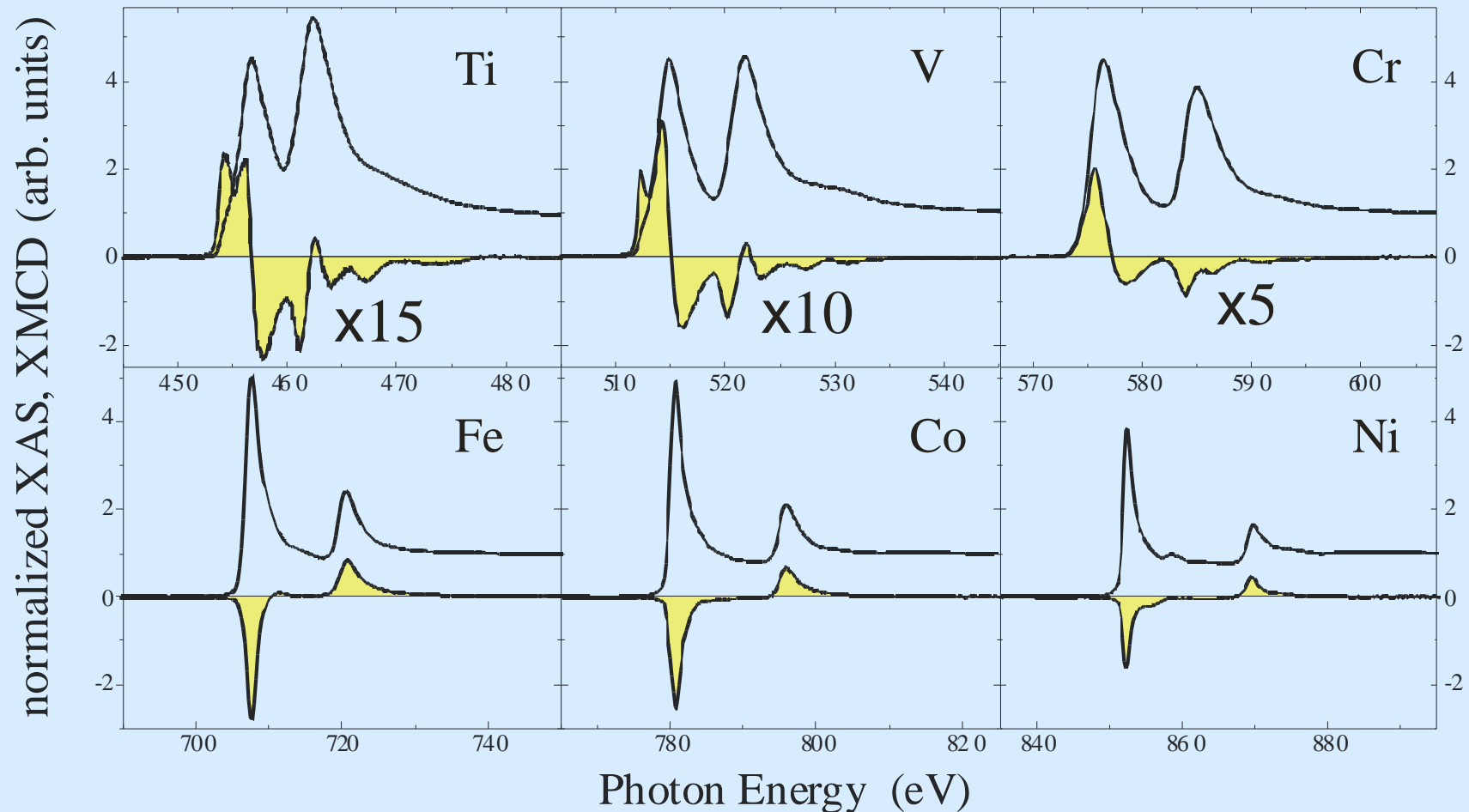
A. Scherz et al., XAFS XII June 2003 Sweden, Physica Scripta;
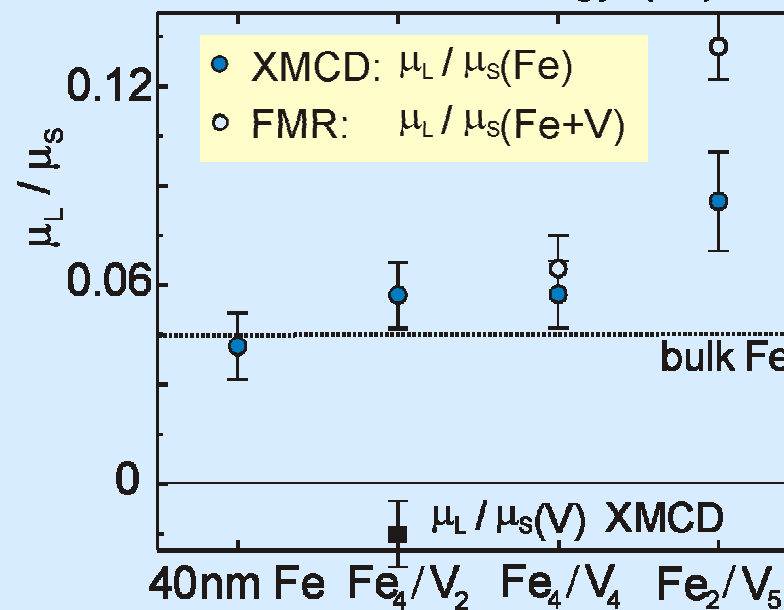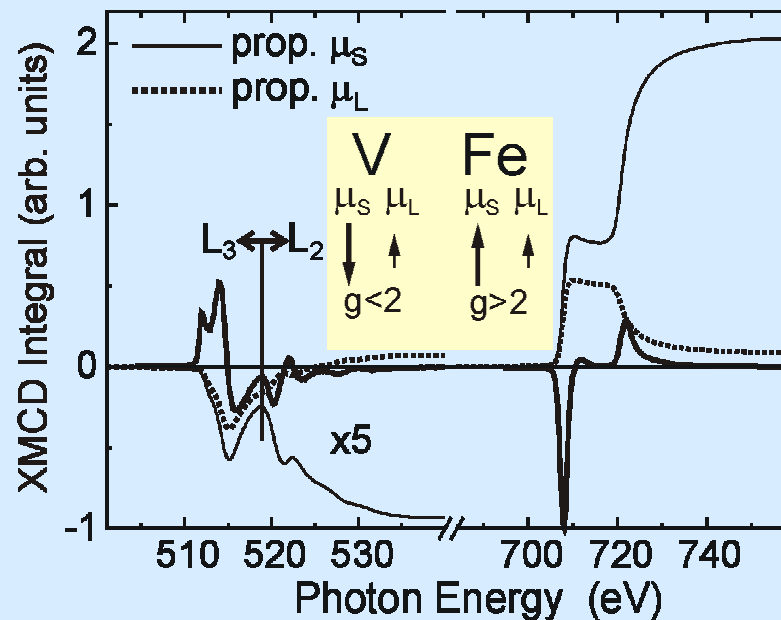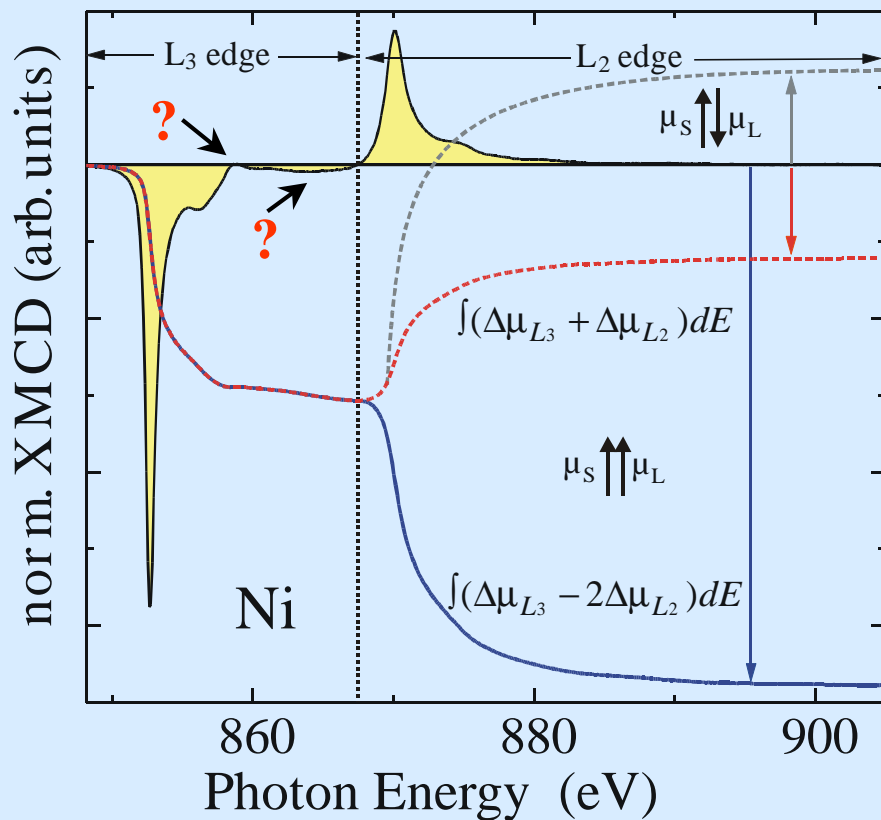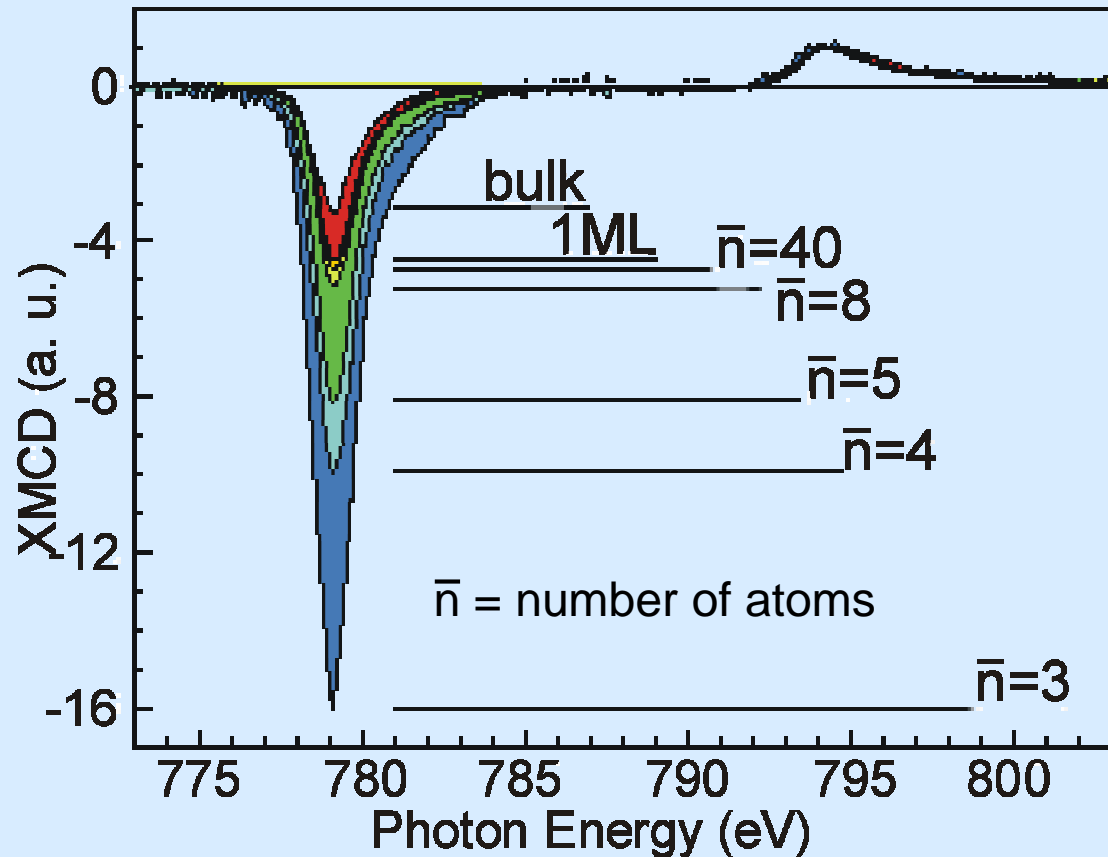A. Scherz et al., BESSY Highlights p. 8 (2002)

X-ray Magnetic Circular Dichroism
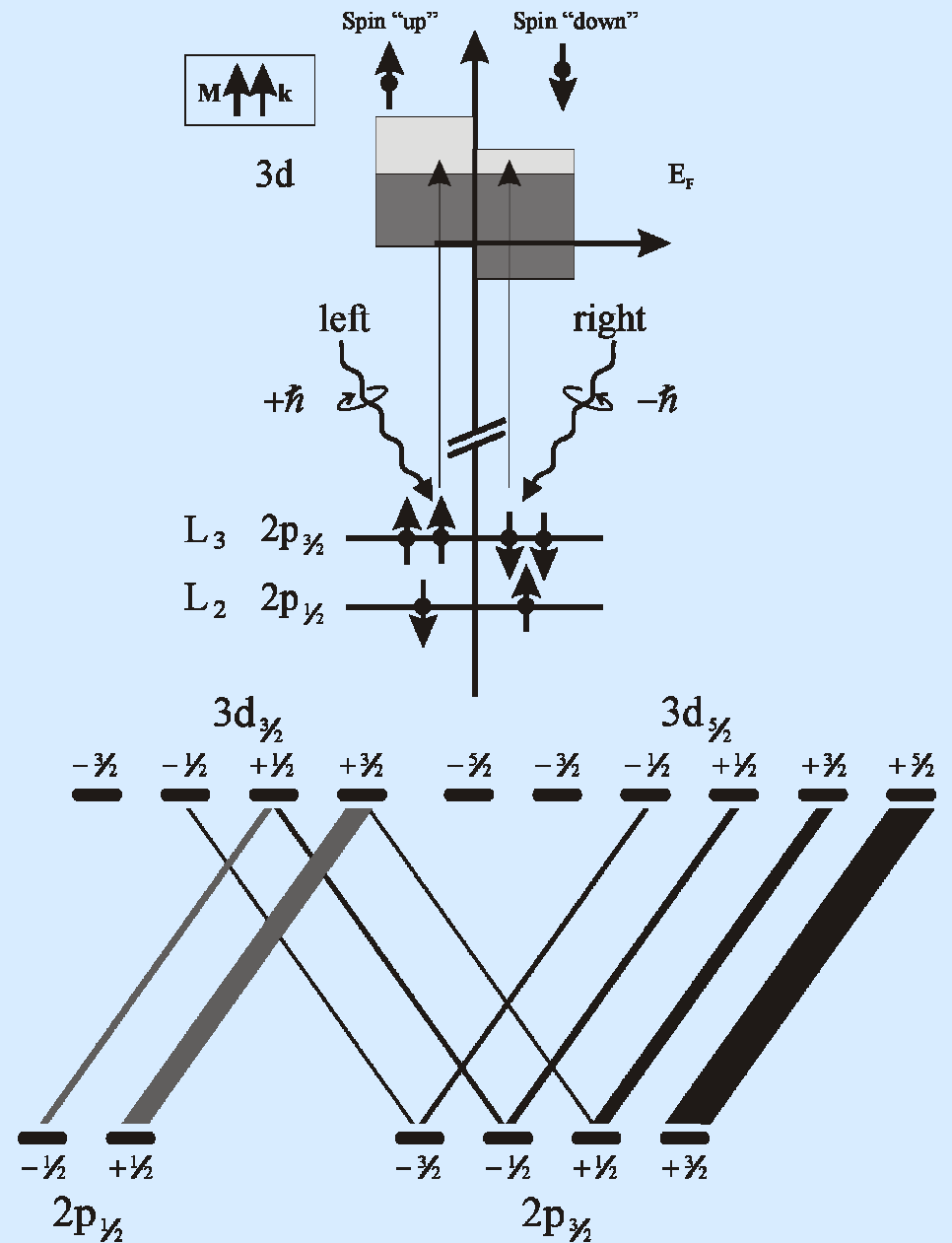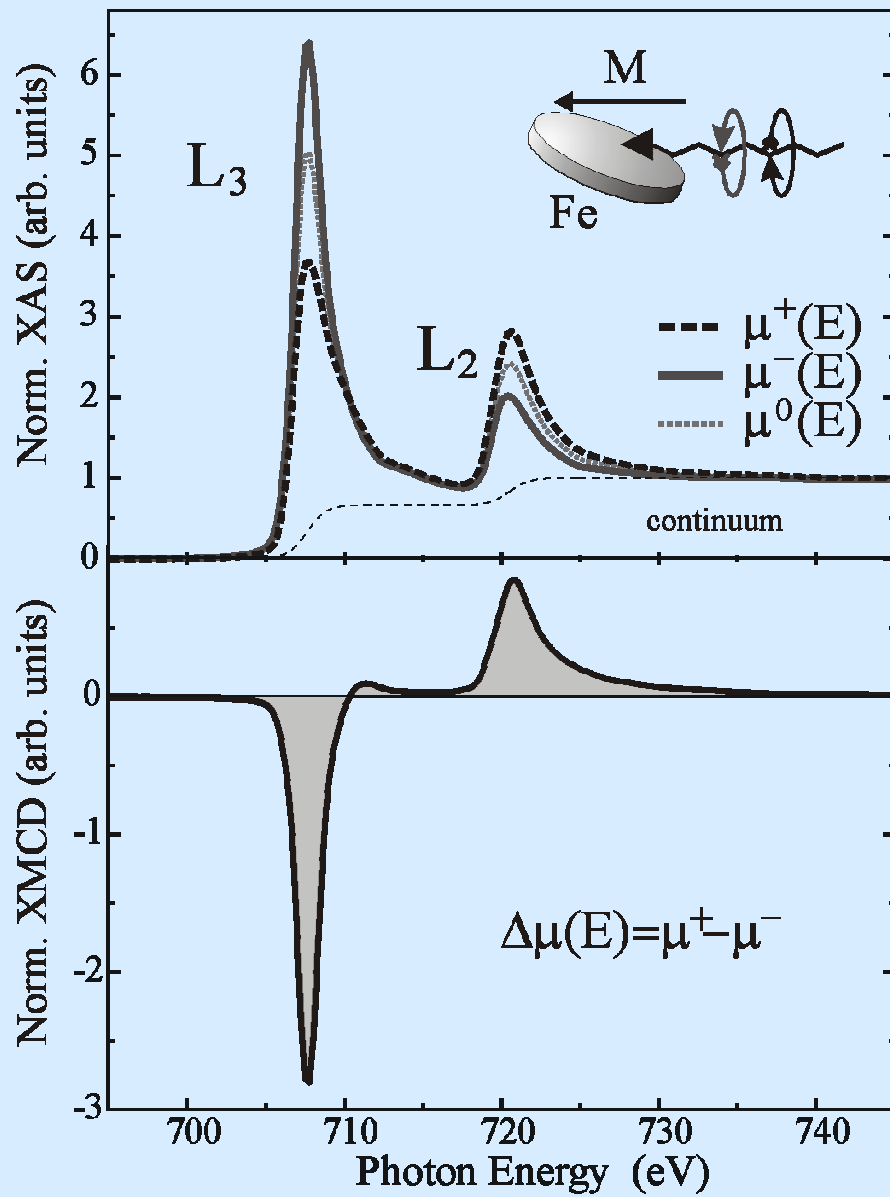
Orbital and spin magnetic moments deduced from XMCD

$$\int \left(\Delta\mu_{L3} - 2 \cdot \Delta\mu_{L2} \right) dE = \frac{N}{3N_h^d} \left(2\langle S_z \rangle^d + 7\langle T_z \rangle^d \right)$$
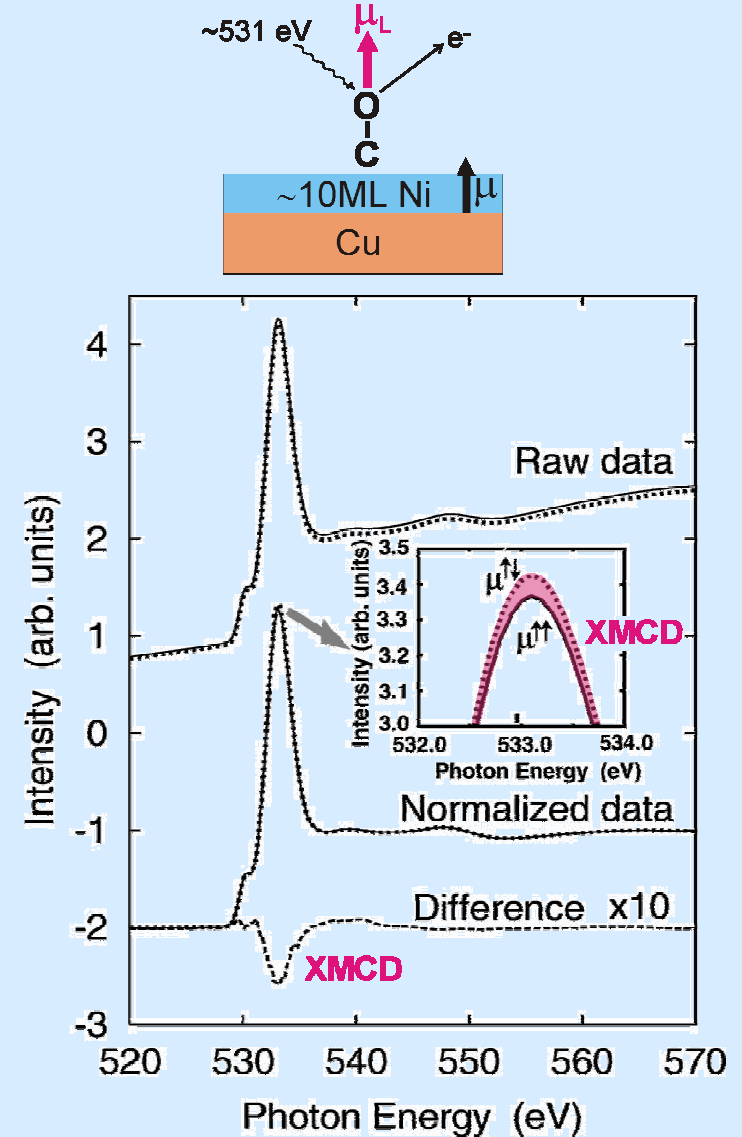
$$\int \left(\Delta\mu_{L3} + \Delta\mu_{L2} \right) dE = \frac{N}{2N_h^d} \langle L_z \rangle^d$$

Giant Magn. Anisotropy of Single Co Atoms and Nanoparticles
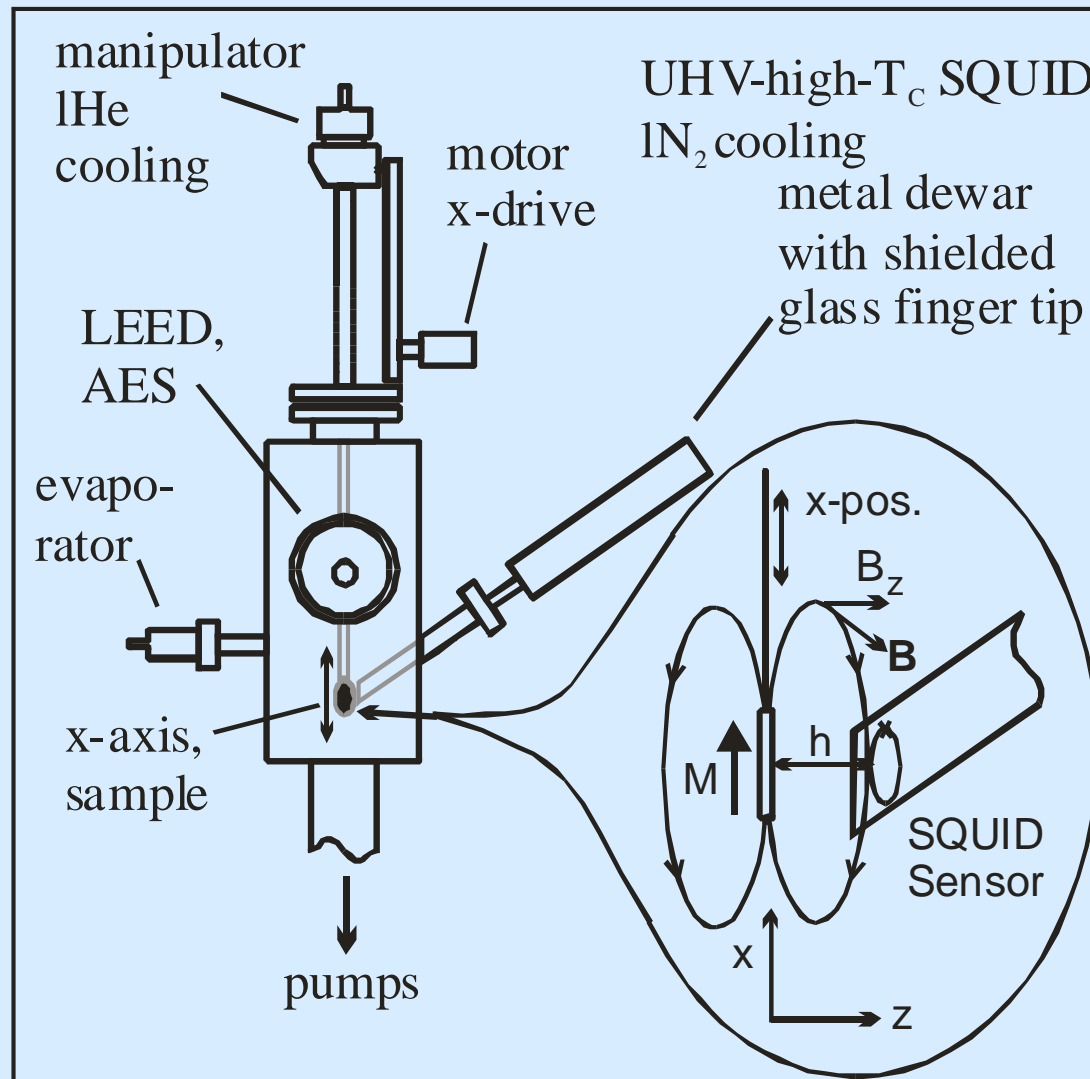
Induced magnetism in molecules

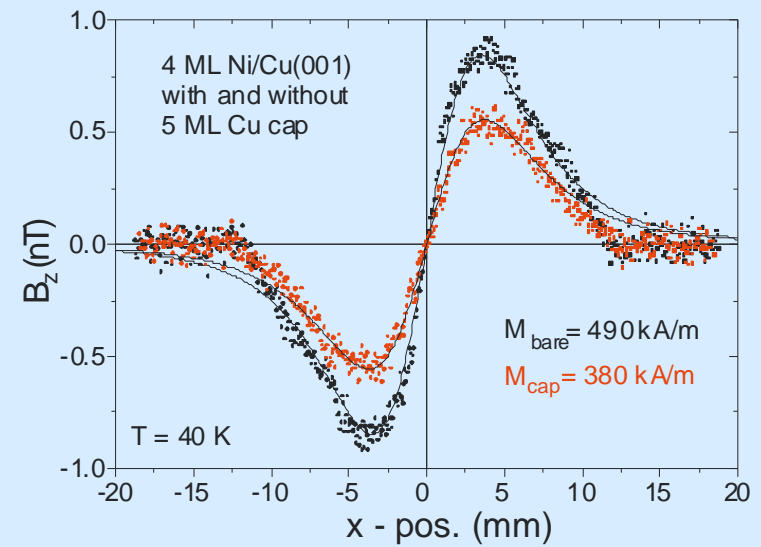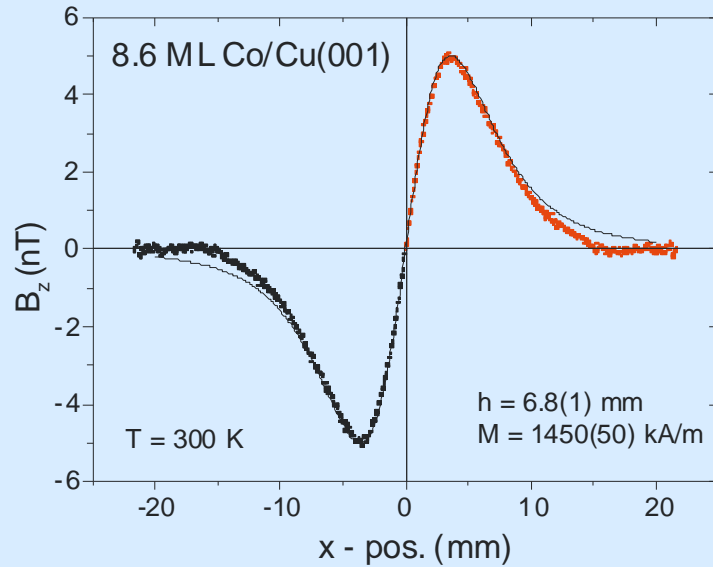P. Gambardella et al., Science **300**, 1130 (2003)

T. Yokoyama et al., PRB **62**, 14191 (2000)

Design of the UHV-SQUID magnetometer

Sensitivity

8.6 ML Co/Cu(001)

B_z (nT)

x - pos. (mm)

T = 300 K

h = 6.8(1) mm
M = 1450(50) kA/m

T = 300 K
h = 4.5 mm
M(bare) = 1395 kA/m
M(cap) = 1100 kA/m

3.1 ML Co/Cu(001)

B_z (nT)

x - pos. (mm)

4 ML Ni/Cu(001)
with and without
5 ML Cu cap

M_{bare} = 490 kA/m

M_{cap} = 380 kA/m

T = 40 K

B_z (nT)

x - pos. (mm)
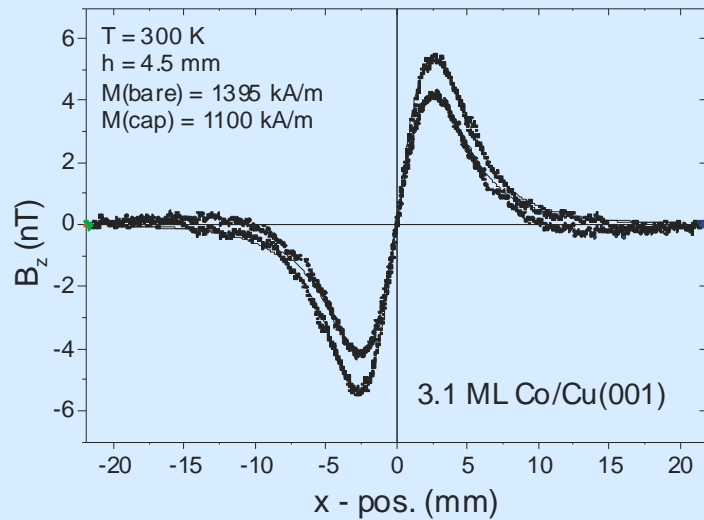
UHV-SQUID measurements
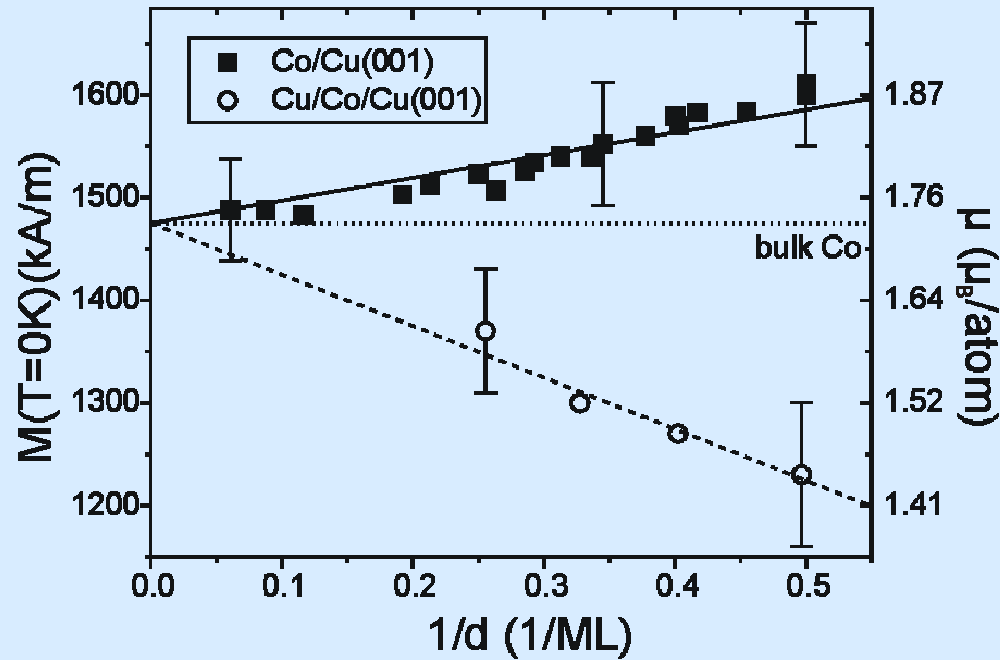
$$m_{tot} = m_{vol} + \frac{m_{surf} + m_{inter} - 2}{d} \quad \text{(linear with 1/d)}$$
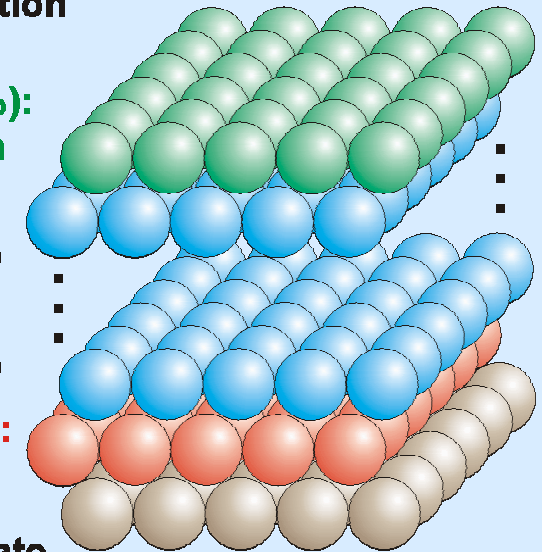
Co moment distribution

Surface (+32(5)%):
2.28(8) μ_B/atom

bulk
μ=1.73μ_B

Interface (-17(3)%):
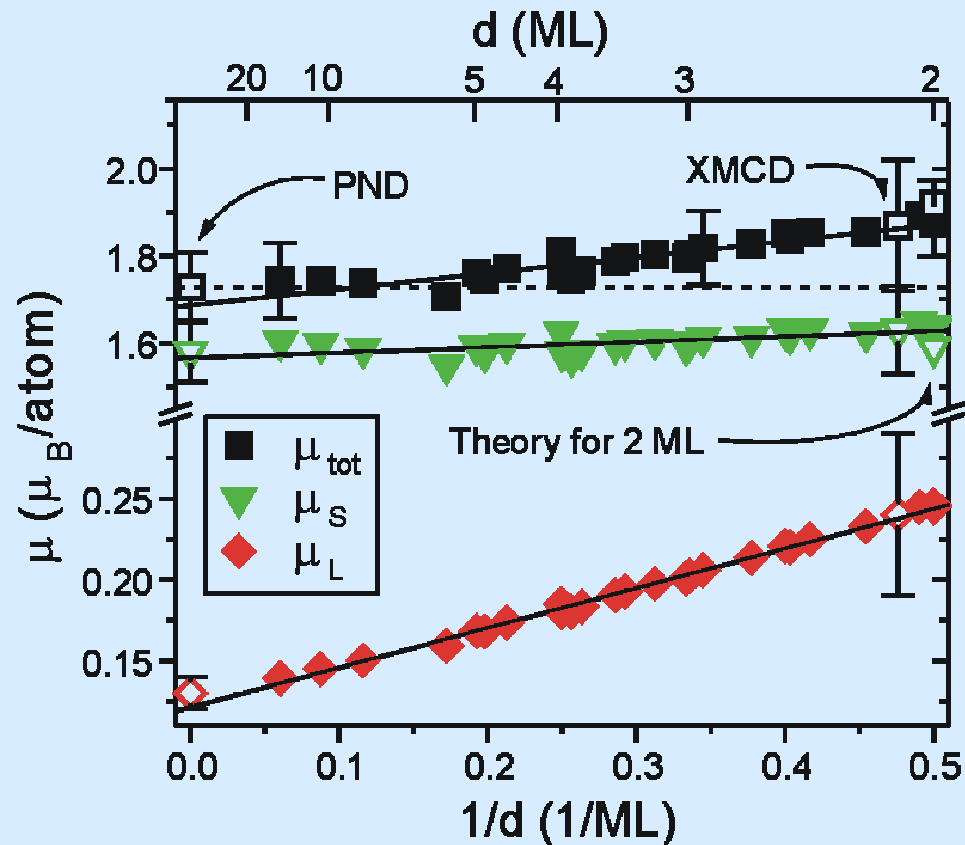1.43(5) μ_B/atom

Cu substrate

Theory:

Hjortstam et al., PRB **53**, 9204 (1996)
Pentcheva et al., PRB **61**, 2211 (2000)

A. Ney et al.
Europhys. Lett. **54**, 820 (2001)

SQUID data deconvolution into spin (μ_S) and orbital (μ_L) moments

The total magnetic moment (squares) of Co/Cu(001) vs the inverse film thickness and its separation into spin (down triangle) and orbital (diamonds) contribution. The bulk value is indicated (dashed line) For comparison experimental results using PND and XMCD are given by the open symbols.

http://www.dissertation.de/PDF/an452.pdf

The effect of temperature

The magnetization of Co/Cu(001) vs the inverse film thickness at different temperatures. The bulk values for 4K (full line) and 300K (dashed line) are indicated.

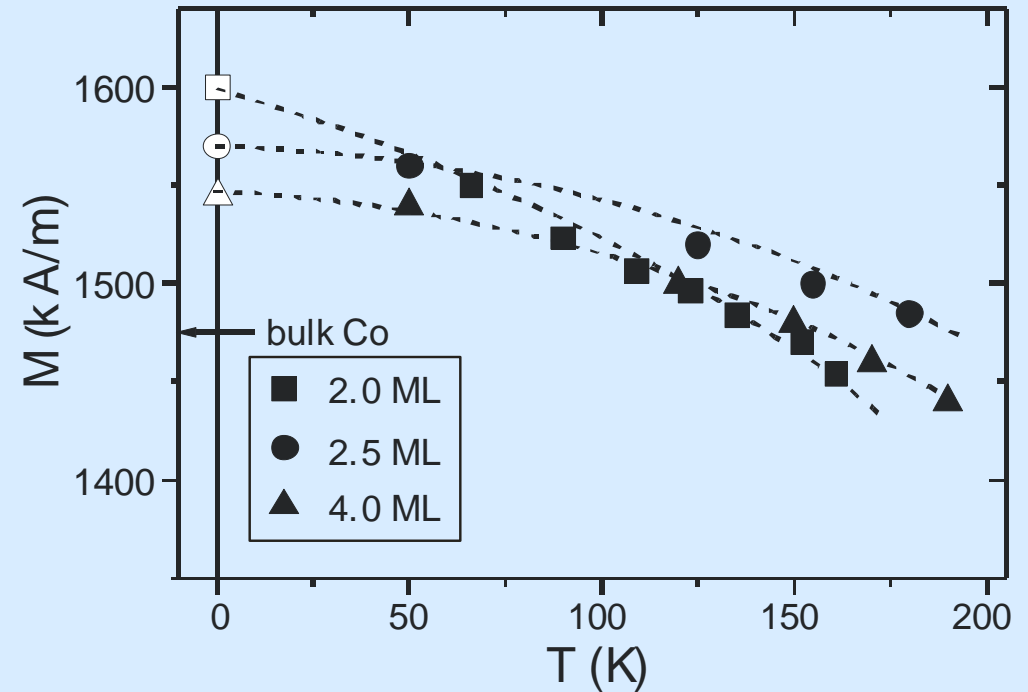# Deconvolution into spin (μ_S) and orbital (μ_L) moments
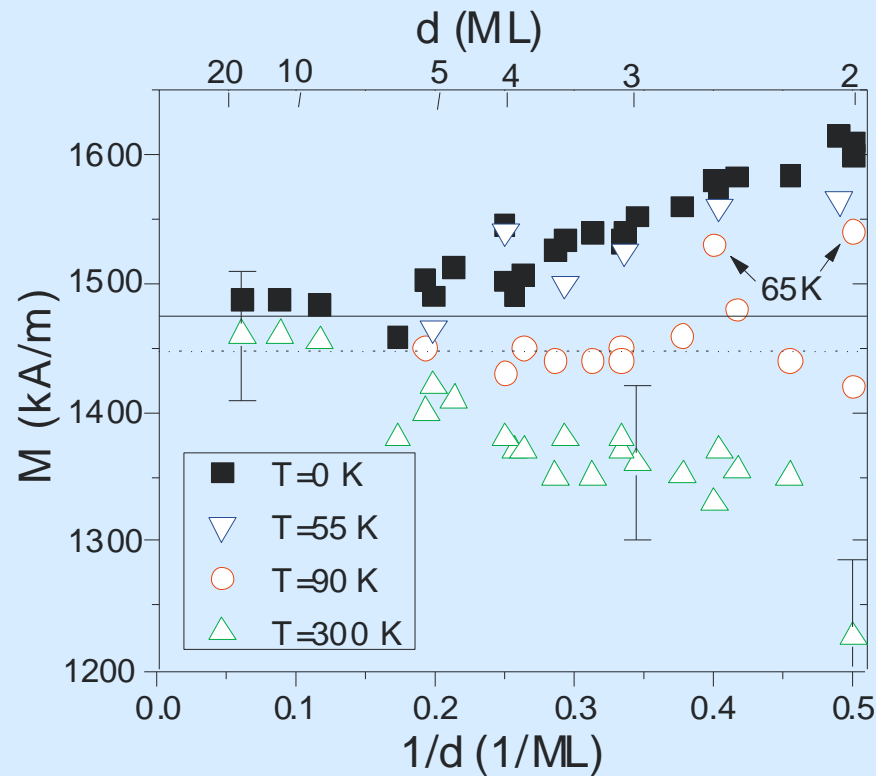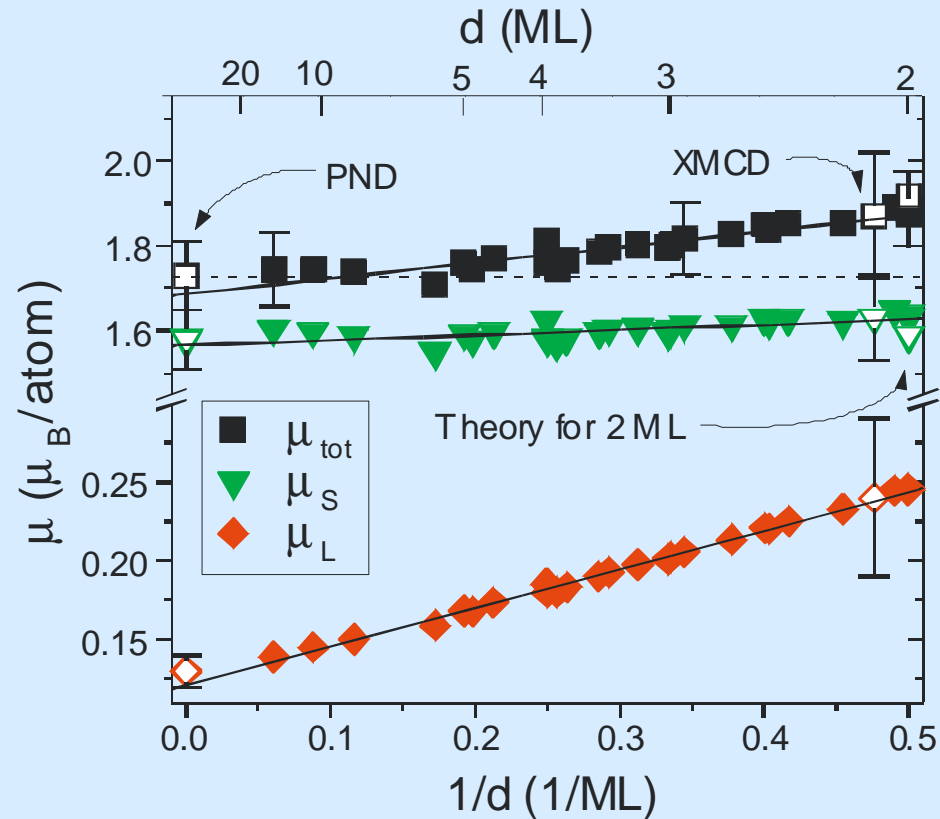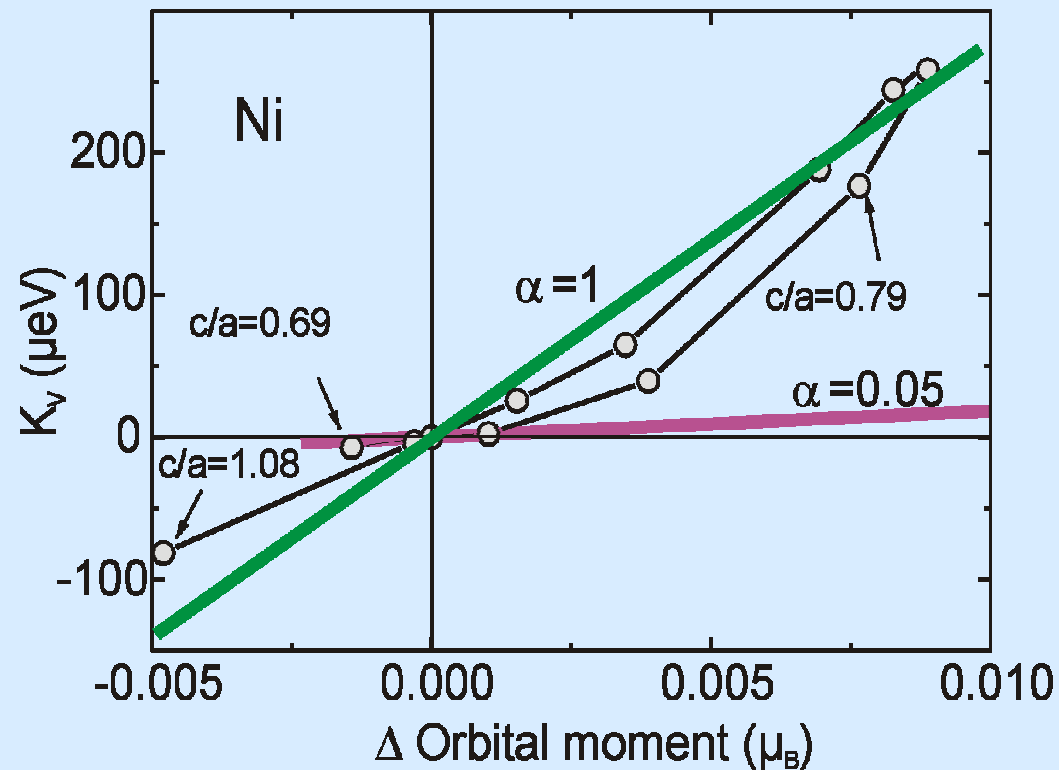

The total magnetic moment (squares) of Co/Cu(001) vs the inverse film thickness and its separation into spin (down triangle) and orbital (diamonds) contribution. The bulk value is indicated (dashed line). For comparison experimental results using PND and XMCD are given by the open symbols.

http://www.dissertation.de/PDF/an452.pdf

Combination of MAE and $\Delta\mu_L$

O. Hjortstam, K. B. et al. PRB **55**, 15026 ('97)
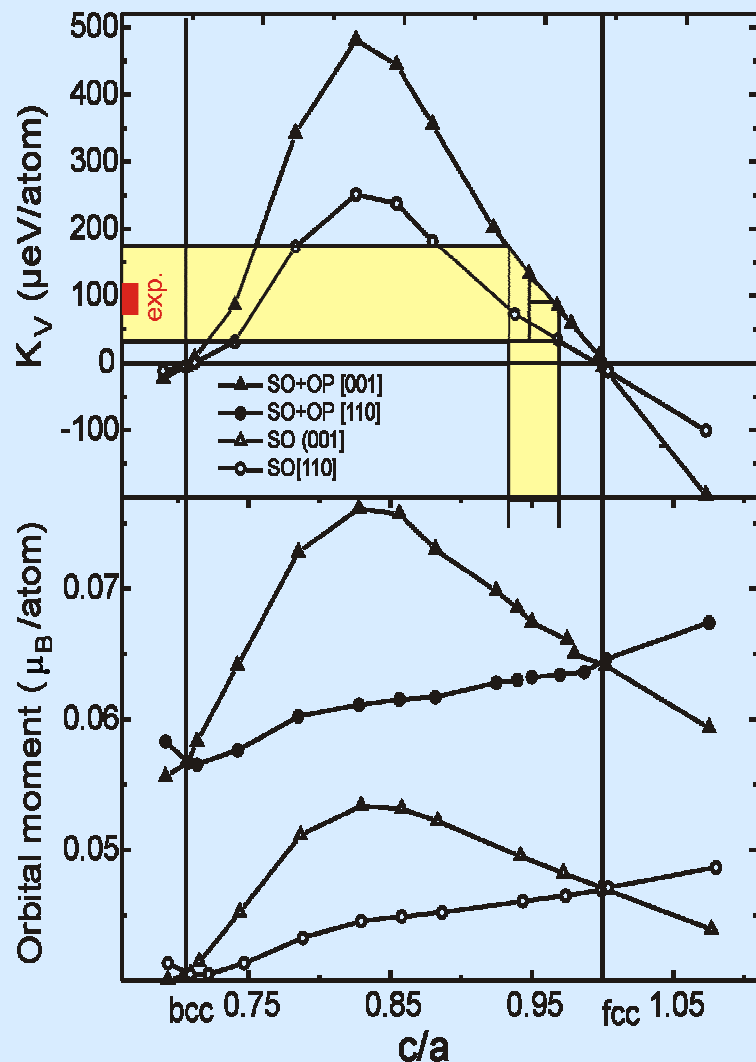
The equ. $\mathrm{MAE} = -\alpha \dfrac{\lambda}{4\mu_B} \Delta\mu_L$ (Bruno `89)

is not strictly a linear relation

Summary of Chap. 3

- Different experiments measure different moments (μ_L and/or μ_S).
  Not every number is a "spin moment".

- FMR was little used, but determines unambiguously the ratio μ_L/μ_S (-if possible!).

- XMCD did use the sum rules very intensely. However, if one looks for small
  contributions of μ_L there are several pitfalls.

- To look at $\Delta\mu_L$ is even worse. At present there is still a mystery: if XMCD measures
  $\Delta\mu_L$ and calculates from this (via „Bruno formula") the MAE, it becomes in most
  cases **to large by a factor 30**.

- SQUID measures in absolute units. But how do we normalize to moments / ion ?
  Apparent enhanced moments appear if a fraction of the ions in a nanocluster do not
  contribute to the magnetization (oxidized, etc.)

Zusatz:

1) „magnetisches Moment"/Atom, gemessen in μ_B, ist temperaturunabhängig.

2) Magnetisierung $M=\Sigma\mu_i$; maximaler Wert = Sättigungsmagnetisierung
   M ist f(T) und verschwindet bei T_C, T_N .

3) μ setzt sich aus μ_L und μ_S zusammen, μ_S ist isotrop, μ_L anisotrop (nicht sphärische
   Ladungsverteilung, Bahndrehimpuls) in Festkörper g-Tensor.

4) Aus 3) resultiert MAE, (makroskopisch: Koerzitivfeldstärke).
   Es gibt (nach meiner Kenntnis) keinen isotropen Heisenberg
   Ferromagneten – mindestens tritt die anisotrope Dipol-Dipol Ww. auf.

5) $J\bar{S}_1 \cdot \bar{S}_2$ ist isotrop, koppelt <u>nicht</u> an den Ortsraum. $(\bar{\mu}_1 \cdot \bar{r})(\bar{\mu}_2 \cdot \bar{r})$ koppelt an $\bar{r}$
   und ist in der Regel anisotrop (siehe $\bar{l} = \bar{r} \times \bar{p}$).

*) bei sogenannten anisotropen Austausch ist $\bar{l}$ via $\lambda\bar{l} \cdot \bar{s}$ in einem effectiven Spinraum
   projeziert